

## Additive Effects of Amines on Asymmetric Hydrogenation of Quinoxalines Catalyzed by Chiral Iridium Complexes

Takuto Nagano,<sup>[a]</sup> Atsuhiko Imuro,<sup>[a]</sup> Rino Schwenk,<sup>[b]</sup> Takashi Ohshima,<sup>[c]</sup>  
Yusuke Kita,<sup>[a]</sup> Antonio Togni,<sup>[b]</sup> and Kazushi Mashima\*<sup>[a]</sup>



**Abstract:** The additive effects of amines were realized in the asymmetric hydrogenation of 2-phenylquinoxaline, and its derivatives, catalyzed by chiral cationic dinuclear triply halide-bridged iridium complexes  $[[\text{Ir}(\text{H})(\text{diphosphine})]_2(\mu\text{-X})_3]\text{X}$  (diphosphine = (*S*)-2,2'-bis(diphenylphosphino)-1,1'-binaphthyl [(*S*)-BINAP], (*S*)-5,5'-bis(diphenylphosphino)-4,4'-bi-1,3-benzodioxole [(*S*)-SEGPHOS], (*S*)-5,5'-bis(diphenylphosphino)-2,2,2',2'-tetrafluoro-4,4'-bi-1,3-benzodioxole [(*S*)-DI-FLUORPHOS]; X = Cl, Br, I) to produce the corresponding 2-aryl-1,2,3,4-tetrahydroquinoxalines. The additive effects of amines were investigated by solution dynamics studies of iridium complexes in the presence of *N*-methyl-*p*-anisidine (MPA), which was determined to be the best amine addi-

tive for achievement of a high enantioselectivity of (*S*)-2-phenyl-1,2,3,4-tetrahydroquinoxaline, and by labeling experiments, which revealed a plausible mechanism comprised of two cycles. One catalytic cycle was less active and less enantioselective; it involved the substrate-coordinated mononuclear complex  $[\text{IrHCl}_2(2\text{-phenylquinoxaline})(\text{S-BINAP})]$ , which afforded half-reduced product 3-phenyl-1,2-dihydroquinoxaline. A poorly enantioselective disproportionation of this half-reduced product afforded (*S*)-2-phenyl-1,2,3,4-tetrahydroquinoxaline. The other cycle involved a more active hy-

dride–amide catalyst, derived from amine-coordinated mononuclear complex  $[\text{IrCl}_2\text{H}(\text{MPA})(\text{S-BINAP})]$ , which functioned to reduce 2-phenylquinoxaline to (*S*)-2-phenyl-1,2,3,4-tetrahydroquinoxaline with high enantioselectivity. Based on the proposed mechanism, an Ir<sup>I</sup>-JOSIPHOS (JOSIPHOS = (*R*)-1-[(*S*<sub>p</sub>)-2-(dicyclohexylphosphino)ferrocenylethyl]diphenylphosphine) catalyst in the presence of amine additive resulted in the highest enantioselectivity for the asymmetric hydrogenation of 2-phenylquinoxaline. Interestingly, the reaction rate and enantioselectivity were gradually increased during the reaction by a positive-feedback effect from the product amines.

**Keywords:** asymmetric catalysis • hydrogenation • iridium • nitrogen heterocycles • reaction mechanisms

## Introduction

Catalytic asymmetric hydrogenation of prochiral unsaturated compounds, which include C=C, C=O, and C=N bonds, has been intensively investigated as a highly versatile and environmentally benign process for creation of a chiral carbon center.<sup>[1]</sup> Asymmetric hydrogenation of N-heteroaromatic compounds is considered to be a difficult task due to aromatic resonance stability. Recent developments in asymmetric hydrogenation of N-heteroaromatic compounds,<sup>[2]</sup> such as 2-substituted quinolines<sup>[3–15]</sup> and quinoxalines<sup>[3h,k,4c,f,11,16–22]</sup> (to give the 1,2,3,4-tetrahydroquinoline and 1,2,3,4-tetrahydroquinoxaline derivatives, respectively, in high enantioselectivity), pyridine derivatives,<sup>[3h,4g,23]</sup> pyr-

roles,<sup>[24]</sup> imidazole,<sup>[25]</sup> oxazole,<sup>[25]</sup> and indoles,<sup>[26]</sup> have been remarkable. However, only a few mechanistic studies of the asymmetric hydrogenation of N-heteroaromatics have been reported. Almost all of the proposed methods for hydrogenation of quinolines assume inner-sphere<sup>[27]</sup> rather than outer-sphere coordination<sup>[4e,15]</sup> of the substrate. In the case of quinoxalines, only one mechanistic study has been reported; Zhou proposed the convergent asymmetric disproportionation of dihydroquinoxalines induced by chiral phosphoric acid in a Ru/Brønsted acid catalyzed asymmetric hydrogenation of 2-aryl quinoxalines.<sup>[21]</sup>

A number of published reports document the dramatic impact of additives on catalytic turnover and enantioselectivity.<sup>[28]</sup> Additive effects are also crucial for asymmetric hydrogenation of N-heteroaromatics. For example, Zhou reported that an iodine source used as an additive to activate the catalyst for asymmetric hydrogenation of imine substrates to give the corresponding chiral amines<sup>[29]</sup> enhanced both the catalytic activity and enantioselectivity.<sup>[3a]</sup> Since then, a rapidly increasing number of effective ligands have been introduced by other groups.<sup>[3f,j,4f,g,9,10]</sup> Other approaches to activate the substrate have also been reported. Zhou studied chloroformate as activators, which acted by the formation of quinolinium and isoquinolinium salts *in situ*; these salts were then smoothly hydrogenated.<sup>[3c]</sup> Feriniga and co-workers reported that addition of piperidine hydrochloride improved the enantioselectivity in the asymmetric hydrogenation of quinolines,<sup>[8]</sup> and Fan and Zhou independently reported that Brønsted acids showed positive effects in the asymmetric hydrogenation of quinolines.<sup>[3i,4e,5b,c]</sup>

As part of our continued interest in the asymmetric hydrogenation of quinoxalines,<sup>[20]</sup> we discovered that the addi-

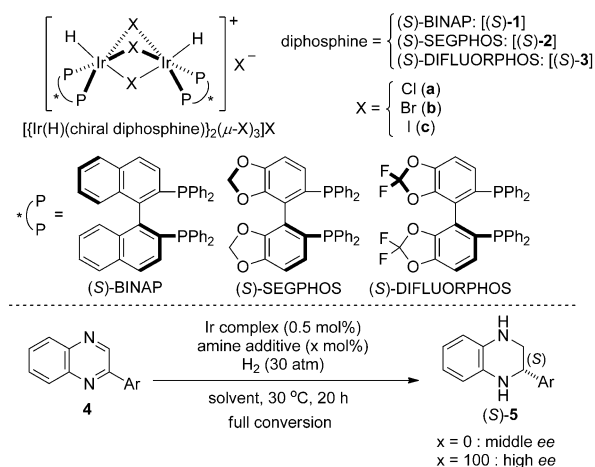
[a] T. Nagano, A. Iimuro, Dr. Y. Kita, Prof. Dr. K. Mashima  
Department of Chemistry  
Graduate School of Engineering Science  
Osaka University, CREST  
Toyonaka, Osaka 560-8631 (Japan)  
Fax: (+81)6-6850-6245  
E-mail: Mashima@chem.es.osaka-u.ac.jp

[b] R. Schwenk, Prof. Dr. A. Togni  
Department of Chemistry and Applied Biosciences  
Swiss Federal Institute of Technology  
ETH Zürich, 8093 Zürich (Switzerland)

[c] Prof. Dr. T. Ohshima  
Graduate School of Pharmaceutical Sciences  
Kyushu University, CREST  
Maidashi Higashi-ku, Fukuoka 812-8582 (Japan)

Supporting information for this article is available on the WWW under <http://dx.doi.org/10.1002/chem.201201366>.

tion of *N*-methylaniline derivatives enhanced not only the catalytic activity but also the enantioselectivity in the generation of 1,2,3,4-tetrahydroquinoxaline derivatives (Scheme 1). Although the additive effects of amines in



Scheme 1. Amine additive effects in the asymmetric hydrogenation of 2-substituted quinoxalines **4** catalyzed by dinuclear iridium complexes **1–3**.

asymmetric hydrogenation of C=N or C=C bonds were previously reported independently by the groups of Tani,<sup>[30]</sup> Bartok,<sup>[31]</sup> and Sugimura,<sup>[32]</sup> the mechanisms of the additive effect of the amine have not been clarified. The present study reveals a dual mechanism that involves equilibrium between two separate catalytic cycles, in which *N*-methylaniline derivatives induce the evolution of the original catalytically active species to a more active and more enantioselective metal–amide catalyst generated through coordination of the amine and elimination of HCl. Herein, we report an efficient hydrogenation of quinoxalines in the presence of an amine additive and our mechanistic studies on the effects of the additive.

## Results and Discussion

**Effects of amine additives:** We examined the additive effects of alkyl and aryl amines (110 mol% relative to the substrate) on the asymmetric hydrogenation of **4a** promoted by BINAP catalyst (*S*-**1a**) under standard reaction conditions [*S*-**1a** (0.5 mol%), 30 atm, 30 °C, 20 h, 1,4-dioxane] and the results are summarized in Table 1. Addition of aniline and tetrahydroquinoline effectively improved the enantioselectivity (63 and 72% *ee*, respectively; Table 1, entries 2 and 3), whereas *n*-hexyl amine and piperidine completely stopped the hydrogenation of **4a** (Table 1, entries 8 and 9). Among aniline and its derivatives, the effects of electron-poor 4-trifluoromethylaniline did not differ from those of unsubstituted aniline (Table 1, entries 5 and 2), but electron-rich 4-methoxyaniline slightly increased the enantioselectivity, although the reaction rate was slower (Table 1, entry 4). In

Table 1. Additive effects of various amines in the asymmetric hydrogenation of **4a**.

Entry	Amine	p <i>K</i> <sub>a</sub>	Conversion [%] <sup>[a]</sup>	<i>ee</i> of ( <i>S</i> )- <b>5a</b> [%] <sup>[b]</sup>
1	–	–	> 99	59
2		4.58	> 99	63
3		4.7	> 99	72
4		5.61	74	74
5		2.57	> 99	63
6		5.93	> 99	85
7		5.85	> 99	77
8		10.7	no reaction	–
9		11.3	no reaction	–

[a] Determined by <sup>1</sup>H NMR analysis of the crude product. [b] Determined by HPLC analysis (Chiralcel OD-H column).

the reaction with *N*-methyl-*p*-anisidine (MPA) as an additive, enantioselectivity was dramatically improved to 85% *ee* with complete conversion of **4a** (Table 1, entry 6). Enantioselectivity was similarly enhanced by 4-methoxy-*N,N*-dimethylaniline (Table 1, entry 7), but to a lesser extent than by MPA. The p*K*<sub>a</sub> value of these amines was clearly crucial for activation of the iridium catalyst. Aromatic amines with a p*K*<sub>a</sub> around 5 not only enhanced the catalytic activity but also improved enantioselectivity for the asymmetric hydrogenation of **4a**, whereas highly basic alkyl amines with a p*K*<sub>a</sub> around 10 seemed to deactivate the iridium species, possibly due to strong coordination to the iridium center. These findings are consistent with reports that simple pyridines and isoquinolines could not be efficiently hydrogenated by similar iridium catalyst systems because their respective hydrogenated cyclic amines would have a p*K*<sub>a</sub> around 10, thus coordinate to, and deactivate, the catalytically active species.<sup>[3c, 23e, g]</sup> Consequently, we selected MPA as the best amine additive for this reaction.

Next, we evaluated the relationship between the amount of MPA and the enantioselectivity under the same reaction conditions; the results are presented in Figure 1. At least 100 mol% of MPA was necessary to adequately enhance the enantioselectivity (84% *ee*). Although use of 110 and 200 mol% of MPA afforded 85 and 87% *ee*, respectively, we fixed the amount of MPA at 100 mol% for subsequent reactions. These observations are consistent with the time de-

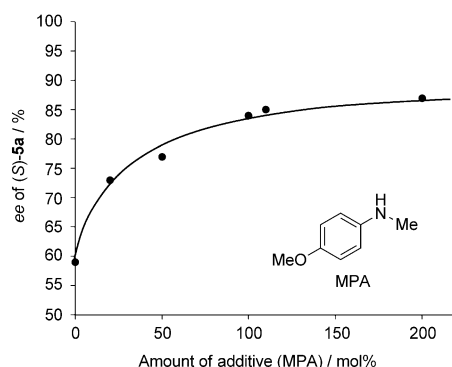
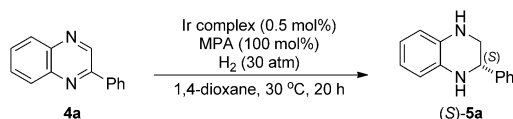


Figure 1. Plot of the amount of additive amine (MPA) versus *ee* of (*S*)-**5a** in the asymmetric hydrogenation of **4a** [(*S*)-**1a** (0.5 mol %), H<sub>2</sub> (30 atm), 30 °C, 20 h, 1,4-dioxane].

pendence of the reaction, in which enantioselectivity increased exponentially with the increasing amount of the amine used (see below).

**Halide and diphosphine ligand effects in (*S*)-BINAP, (*S*)-SEGPHOS, and (*S*)-DIFLUORPHOS complexes:** In the presence of the optimized amine additive MPA (100 mol %), (*S*)-BINAP, (*S*)-SEGPHOS, and (*S*)-DIFLUORPHOS iridium complexes (*S*)-**1a–c**, (*S*)-**2a–c**, and (*S*)-**3a–c** (Scheme 1) with different halide ligands (chloride, bromide, and iodide) were tested as catalysts for the hydrogenation of **4a** at 30 °C and the results are shown in Table 2. Among the tested atropisomeric chiral chelating diphosphine ligands, (*S*)-DIFLUORPHOS complexes **3** were superior relative to the respective (*S*)-BINAP and (*S*)-SEGPHOS complexes **1** and **2**. Chloro complexes (*S*)-**1a**, (*S*)-**2a**, and (*S*)-**3a** afforded the hydrogenated product (*S*)-**5a** with better enantioselectivity

Table 2. Catalytic performance of chloro, bromo, and iodo iridium complexes with (*S*)-BINAP, (*S*)-SEGPHOS, and (*S*)-DIFLUORPHOS ligands.



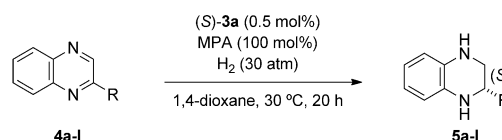
Entry	Diphosphine	X	Conversion [%] <sup>[a]</sup>	<i>ee</i> of ( <i>S</i> )- <b>5a</b> [%] <sup>[b]</sup>
1		Cl ( <b>3a</b> )	> 99	93
2		Br ( <b>3b</b> )	> 99	89
3		I ( <b>3c</b> )	> 99	81
4		Cl ( <b>2a</b> )	> 99	88
5		Br ( <b>2b</b> )	> 99	86
6		I ( <b>2c</b> )	> 99	81
7		Cl ( <b>1a</b> )	> 99	84
8		Br ( <b>1b</b> )	> 99	75
9		I ( <b>1c</b> )	> 99	47

[a] Determined by <sup>1</sup>H NMR analysis of the crude product. [b] Determined by HPLC analysis (Chiralcel OD-H column).

than the analogous bromo- or iodo complexes, which indicated that at least one halide atom was necessary to coordinate to the iridium atom during the reaction. Notably, the requirement for a halide atom bound to the iridium complex is consistent with a report that halide-free iridium complexes show low catalytic activity for asymmetric hydrogenation of imines.<sup>[29]</sup> Such superiority of chloride complexes contrasted with reports that chiral iodo-iridium complexes that bear a chiral diphosphine ligand tend to be the best catalysts among the series of halide complexes for asymmetric hydrogenation of N-heteroaromatic compounds.<sup>[3a,g,j,4f,g,9,10]</sup> Consequently, we selected (*S*)-**3a** combined with MPA (100 mol %) as the best catalyst system.

Under the optimized catalytic conditions [(*S*)-**3a**/MPA], we conducted asymmetric hydrogenation reactions of various 2-arylquinoxalines **4** and the results are summarized in Table 3. *Para*-substituted phenylquinoxalines **4d** and **4g–k**,

Table 3. Asymmetric hydrogenation of 2-arylquinoxalines **4** catalyzed by (*S*)-**3a**/MPA.



Entry	R	<b>4</b>	Conversion [%] <sup>[a]</sup>	<b>5</b>	<i>ee</i> of ( <i>S</i> )- <b>5</b> [%] <sup>[b]</sup>
1	C <sub>6</sub> H <sub>5</sub>	<b>4a</b>	> 99	<b>5a</b>	93
2	<i>o</i> -Me–C <sub>6</sub> H <sub>4</sub>	<b>4b</b>	72 (>99) <sup>[c]</sup>	<b>5b</b>	92 (92) <sup>[c]</sup>
3	<i>m</i> -Me–C <sub>6</sub> H <sub>4</sub>	<b>4c</b>	> 99	<b>5c</b>	90
4	<i>p</i> -Me–C <sub>6</sub> H <sub>4</sub>	<b>4d</b>	> 99	<b>5d</b>	92
5	<i>o</i> -OMe–C <sub>6</sub> H <sub>4</sub>	<b>4e</b>	69 (95) <sup>[c]</sup>	<b>5e</b>	63 (63) <sup>[c]</sup>
6	<i>m</i> -OMe–C <sub>6</sub> H <sub>4</sub>	<b>4f</b>	> 99	<b>5f</b>	92
7	<i>p</i> -OMe–C <sub>6</sub> H <sub>4</sub>	<b>4g</b>	> 99	<b>5g</b>	92
8	<i>p</i> -NO <sub>2</sub> –C <sub>6</sub> H <sub>4</sub>	<b>4h</b>	> 99	<b>5h</b>	92
9	<i>p</i> -F–C <sub>6</sub> H <sub>4</sub>	<b>4i</b>	> 99	<b>5i</b>	93
10	<i>p</i> -Cl–C <sub>6</sub> H <sub>4</sub>	<b>4j</b>	93	<b>5j</b>	91
11	<i>p</i> -Br–C <sub>6</sub> H <sub>4</sub>	<b>4k</b>	> 99	<b>5k</b>	91
12	<i>m</i> -Br–C <sub>6</sub> H <sub>4</sub>	<b>4l</b>	> 99	<b>5l</b>	91

[a] Determined by <sup>1</sup>H NMR analysis of the crude product. [b] Determined by HPLC analysis (Chiralcel OD-H column). [c] Reaction time was 40 h.

which bear an electron-donating group, such as methyl or methoxy, or an electron-withdrawing group, such as a halide or nitro group, were efficiently hydrogenated to give tetrahydroquinoxaline derivatives (*S*)-**5d** and (*S*)-**5g–k**, respectively, with high enantioselectivities (91–93% *ee*; Table 3, entries 4 and 7–11). Furthermore, hydrogenation of *meta*-substituted substrates **4c**, **4f**, and **4l** proceeded smoothly to give (*S*)-**5c**, (*S*)-**5f**, and (*S*)-**5l**, respectively, with high enantioselectivity (90–92% *ee*; Table 3, entries 3, 6 and 12). Steric bulkiness at the *ortho*-position affected the reactivity. *Ortho*-methyl and *ortho*-methoxy substituents reduced the reactivity such that a prolonged reaction time of 40 h was required to complete the reactions (Table 3, entries 2 and 5). *Ortho*-methyl-substituted substrate **4b** resulted in **5b** in high

enantioselectivity (92% *ee*; Table 3, entry 2), whereas *ortho*-methoxy-substituted substrate **4e** remarkably reduced the enantioselectivity to 63% *ee* (Table 3, entry 5), presumably due to chelation of the methoxy group and the nitrogen atom located at the 1-position of quinoxaline to the iridium center.

**Mechanistic study:** Our strong interest in the mechanism of such amine additive effects in the asymmetric hydrogenation of **4a** led us to conduct a mechanistic study by using (*S*)-**1a**, together with (*S*)-**2a** to isolate the intermediate species (due to suitability of SEGPHOS for crystallization), with MPA and *p*-anisidine (PA) as additive amines. The results are described below and a plausible mechanism is illustrated in Figure 2. Two separate catalytic cycles that afforded reduced

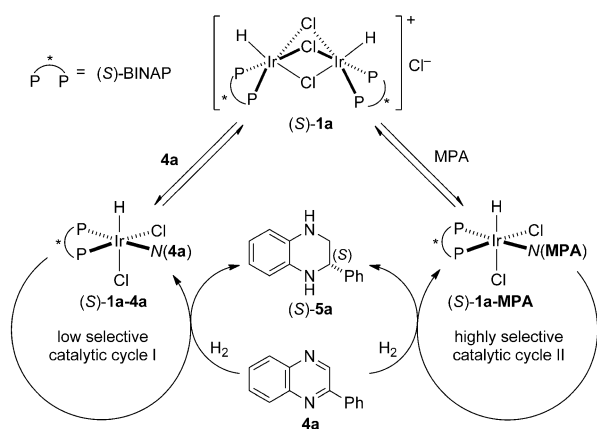
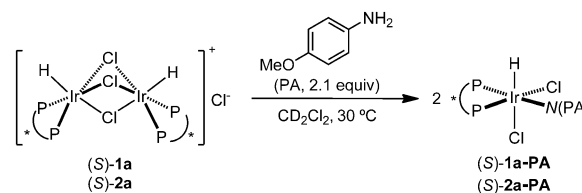


Figure 2. Summary of the reaction mechanism of amine additive effects on the asymmetric hydrogenation of **4a**.

product **5a** in low (cycle I) and high (cycle II) enantioselectivity, respectively, were involved in this catalytic system, and the two catalytic cycles were individually catalyzed by two different active catalytic species, [(*S*)-**1a-4a** and (*S*)-**1a-MPA**], respectively, which were in equilibrium with each other throughout the catalytic reaction. The amount of amine used changed the abundance ratio of the two catalytically active species and large amounts of amine were required to shift the reaction from cycle I to II to improve enantioselectivity over the whole catalytic system. In the following mechanistic study, CD<sub>2</sub>Cl<sub>2</sub> was used as the solvent for the purpose of NMR spectroscopic measurements because the solubility of iridium precursors (*S*)-**1** and (*S*)-**2** was much better in CH<sub>2</sub>Cl<sub>2</sub> than in 1,4-dioxane. The amine additive effects for the asymmetric hydrogenation of **4a** were similar in CH<sub>2</sub>Cl<sub>2</sub> and 1,4-dioxane.<sup>[33]</sup>

**Reaction of (*S*)-**1a** and (*S*)-**2a** with amines and **4a**:** First, we conducted controlled experiments for the addition of MPA (the best additive amine), as well as for PA, (a moderately effective amine additive) to a solution of iridium catalyst (*S*)-**1a** in CD<sub>2</sub>Cl<sub>2</sub> under an argon atmosphere. The reaction

of the dinuclear iridium complex (*S*)-**1a** with PA (2.1 equiv) was monitored by <sup>1</sup>H and <sup>31</sup>P{<sup>1</sup>H} NMR spectroscopy, which confirmed that PA coordinated to the iridium center to give a single isomer of amine adduct (*S*)-**1a-PA** (Scheme 2). The



Scheme 2. Reaction of dinuclear iridium complexes with PA (2.1 equiv).

<sup>1</sup>H NMR spectrum in CD<sub>2</sub>Cl<sub>2</sub> displayed a hydride signal at  $\delta = -20.1$  ppm (dd,  $J(\text{H,P}) = 14.2, 21.4$  Hz); the coupling constant values were consistent with a structure in which hydride is *cis* to the two phosphorus atoms of the BINAP ligand. The <sup>31</sup>P{<sup>1</sup>H} NMR spectrum displayed a pair of doublets at  $\delta = 0.3$  and  $-5.6$  ppm ( $J(\text{P,P}) = 18.6$  Hz). The amine and methoxy protons of PA in (*S*)-**1a-PA** were observed at  $\delta = 4.7$  (brs) and 3.6 ppm (s), respectively. Complex (*S*)-**1a-PA** was isolated as yellow crystalline solid and further characterized by elemental analysis and mass spectroscopy. Notably, the isolated complex (*S*)-**1a-PA** had very low catalytic activity, presumably due to strong coordination of PA to the iridium center and low solubility in the solvent, consistent with the observed low catalytic activity (Table 1, entry 4).

Similar treatment of SEGPHOS complex (*S*)-**2a** with PA afforded complex (*S*)-**2a-PA**, which was characterized by NMR spectroscopy [ $\delta_{\text{H}} = -20.1$  ppm (dd,  $J(\text{H,P}) = 13.9, 21.4$  Hz);  $\delta_{\text{P}} = -0.8$  and  $-7.2$  ppm (d,  $J(\text{P,P}) = 19.1$  Hz)], as well as elemental analysis and mass spectroscopy. Complex (*S*)-**2a-PA** was crystallized from a saturated solution of hexane and CH<sub>2</sub>Cl<sub>2</sub>. Figure 3 shows an ORTEP drawing of (*S*)-**2a-PA**, in which the iridium atom adopts an octahedral geometry. The hydride atom occupies a position *cis* to the two phosphine atoms of SEGPHOS and the nitrogen atom of PA, and the two other positions of the octahedral iridium

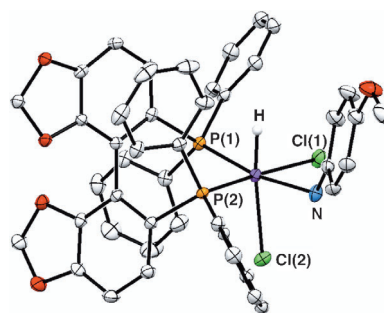
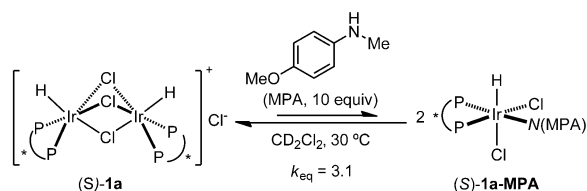


Figure 3. Crystal structure and numbering scheme of (*S*)-**2a-PA**. Selected bond lengths [Å] and angles [°]: Ir–H 1.38(2), Ir–Cl(1) 2.435(5), Ir–Cl(2) 2.499(5), Ir–N 2.181(18), Ir–P(1) 2.275(5), Ir–P(2) 2.256(5); P(1)–Ir–P(2) 92.71(2), P(1)–Ir–H 83(1), P(2)–Ir–H 88(1), P(1)–Ir–N 169.48(5), P(2)–Ir–N 93.62(5), N–Ir–H 89(1). The angle between the best planes of the backbone aromatic carbons of (*S*)-SEGPHOS = 66.02°.

center are occupied by two chloride atoms. The bond length of Ir–P(1) (2.275(5) Å) was 0.02 Å longer than that of Ir–P(2) (2.256(5) Å) due to the influence of the nitrogen atom *trans* to P(1). The anisyl group of PA was oriented upward toward the hydride atom, pointing to the less-bulky environment around the iridium center, and surrounded by the edge and face phenyl groups of the SEGPHOS ligand. Accordingly, the absolute configuration of (S)-SEGPHOS complex (S)-2a-PA was assigned as *OC*-6-42-*C*.

We then measured the  $^1\text{H}$  NMR spectrum of (S)-1a and the best additive MPA (10 equiv) in  $\text{CD}_2\text{Cl}_2$  solution in the temperature range of  $-60$  to  $30^\circ\text{C}$  (Scheme 3 and Figure 4). In the  $^1\text{H}$  NMR spectrum measured at  $-60^\circ\text{C}$ , the amine adduct (S)-1a-MPA was characterized by a doublet of doublets at  $\delta = -19.9$  ppm ( $J(\text{H},\text{P}) = 13.4, 20.8$  Hz) in the hydride region, along with a doublet of doublets due to (S)-1a. The chemical shift value and two coupling constants for (S)-1a-MPA were in good accord with those of (S)-1a-PA, which suggests that (S)-1a-MPA is a mononuclear octahedral complex with an *OC*-6-42-*C* stereochemistry (Scheme 3). Upon warming the solution to  $30^\circ\text{C}$ , the doublet of doublets due to (S)-1a-MPA broadened to give a signal at  $\delta = -20.2$  ppm (br) and the relative intensity of the signal due to (S)-1a increased, which indicated an equilibrium between (S)-1a-MPA and (S)-1a with temperature-dependent equilibrium constants that obeyed the van 't Hoff equation to give  $\Delta H = -0.34(7)$  kJ mol $^{-1}$ . In the  $^{31}\text{P}\{^1\text{H}\}$  NMR spectrum at  $-60^\circ\text{C}$ , a pair of doublets at  $\delta = 3.7$  and  $-3.7$  ppm with  $J(\text{P},\text{P}) = 17.9$  Hz was observed, along



Scheme 3. Reaction of dinuclear iridium complex with MPA (10 equiv).

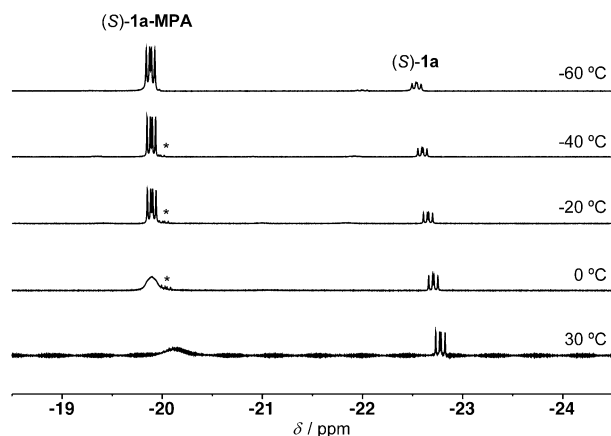
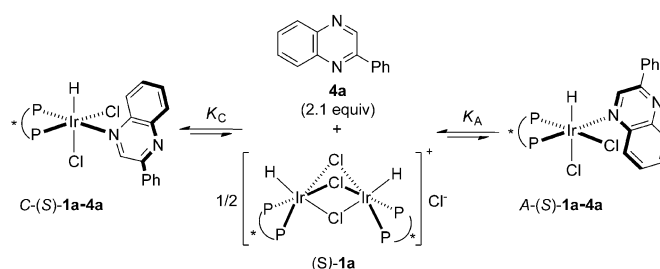


Figure 4.  $^1\text{H}$  NMR spectra of the reaction mixture of (S)-1a and MPA (10 equiv) in the temperature range  $-60$ – $30^\circ\text{C}$  in  $\text{CD}_2\text{Cl}_2$ . Asterisk indicates an impurity.

with a pair of signals due to (S)-1a. Similarly, we observed the formation of (S)-2a-MPA, and an equilibrium between (S)-2a-MPA and (S)-2a. Because of the equilibrium, the amine adducts (S)-1a-MPA and (S)-2a-MPA could not be isolated, however, the starting complexes (S)-1a and (S)-2a were precipitated.

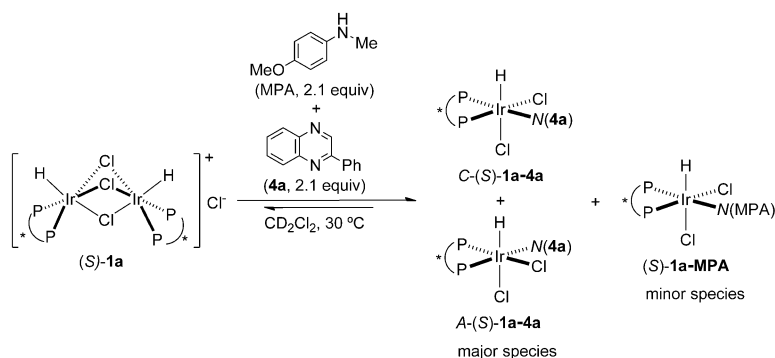
The coordination of PA and MPA to the dinuclear iridium precursor (S)-1a to give the corresponding mononuclear adducts (S)-1a-PA and (S)-1a-MPA prompted us to investigate the coordination of 4a to (S)-1a. Use of NMR spectroscopy to monitor the mixture of (S)-1a and 4a in  $\text{CD}_2\text{Cl}_2$  at  $-40^\circ\text{C}$  revealed two pairs of signals due to stereoisomers of (S)-1a-4a [major:  $\delta_{\text{H}} = -18.2$  ppm (dd,  $J(\text{H},\text{P}) = 12.3, 17.2$  Hz);  $\delta_{\text{P}} = -5.9$  (d,  $J(\text{P},\text{P}) = 19.4$  Hz) and  $-12.9$  ppm (d,  $J(\text{P},\text{P}) = 19.4$  Hz); minor:  $\delta_{\text{H}} = -19.3$  ppm (dd,  $J(\text{P},\text{H}) = 14.2, 21.7$  Hz);  $\delta_{\text{P}} = 2.2$  (d,  $J(\text{P},\text{P}) = 21.2$  Hz) and  $-4.3$  ppm (d,  $J(\text{P},\text{P}) = 21.2$  Hz)] (Scheme 4). The two isomers of the 4a-coordinated iridium complex were assigned as *C*-(S)-1a-4a, *OC*-6-42-*C* (major), and *A*-(S)-1a-4a, *OC*-6-42-*A* (minor). Assignment of the major isomer was assumed based on the crystal structure of (S)-2a-PA and that the coordination of 4a to the iridium center was reversible (see the Supporting Information).<sup>[33]</sup> Equilibrium constants  $K_{\text{C}}$  for (S)-1a and *C*-(S)-1a-4a and  $K_{\text{A}}$  for (S)-1a and *A*-(S)-1a-4a were applied to the van 't Hoff equation and the estimated enthalpies were  $\Delta H_{\text{C}} = -0.67(4)$  kJ mol $^{-1}$  and  $\Delta H_{\text{A}} = -0.42(4)$  kJ mol $^{-1}$ , which indicated that the coordination of 4a was an endothermic process.



Scheme 4. Coordination of 4a to (S)-1a to form iridium complexes *C*-(S)-1a-4a and *A*-(S)-1a-4a.

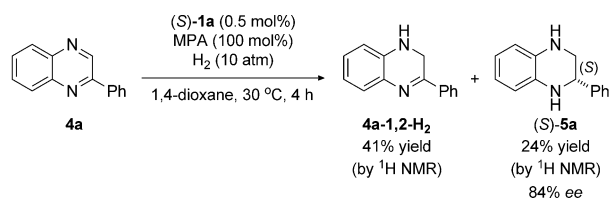
A competition experiment in which (S)-1a was treated with 4a (2.1 equiv) and MPA (2.1 equiv) provided a mixture of the two isomers of (S)-1a-4a together with a minor amount of (S)-1a-MPA based on  $^1\text{H}$  NMR spectroscopic measurements. This indicated that N-heteroaromatic compound 4a coordinated more strongly to the iridium center than MPA (Scheme 5). Accordingly, the difference in the coordination abilities of 4a and MPA was precisely why such a large amount (100 mol %) of MPA was needed to shift the equilibrium in favor of (S)-1a-MPA to improve the enantioselectivity in cycle II (Figure 2).

**Cycle I, catalyzed by (S)-1a-4a:** When the asymmetric hydrogenation of 4a promoted by (S)-1a and additive MPA (100 mol %) was stopped after a short reaction time (4 h),



Scheme 5. Competition reaction of (S)-1a with MPA (2.1 equiv) and 4a (2.1 equiv).

hydrogenated product (S)-5a was obtained in low yield (24%) and high enantioselectivity (84% ee). Furthermore, at partial conversion of 4a, 3-phenyl-1,2-dihydroquinoxaline (4a-1,2-H<sub>2</sub>) was detected in 41% yield (Scheme 6). When

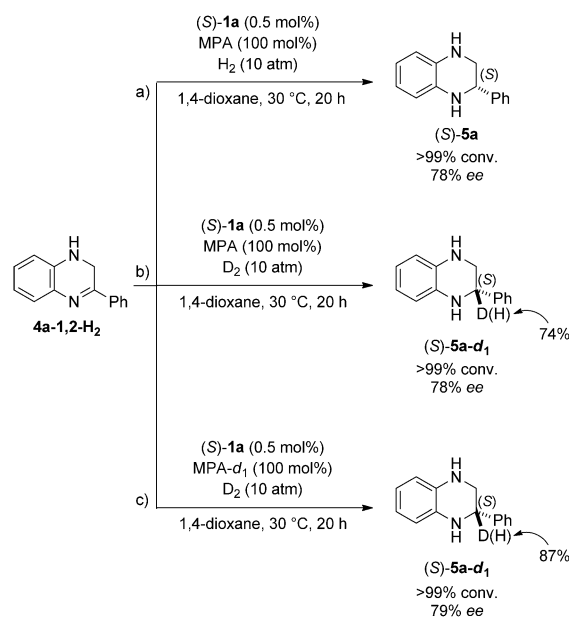


Scheme 6. Asymmetric hydrogenation of 4a with short reaction times.

the hydrogenation reaction of 4a-1,2-H<sub>2</sub> was performed under D<sub>2</sub> (10 atm), (S)-5a-d<sub>1</sub> was obtained with the same enantiomeric excess (78% ee) and the deuterium content at the 2-position of (S)-5a-d<sub>1</sub> was determined to be 74% based on <sup>1</sup>H NMR spectroscopic measurements (Scheme 7b). The deuterium content at the 1-position (amine proton) could not be determined due to scrambling and broadening of the signal. This partial deuterium incorporation at the 2-position was explained by the assumption of the existence of an extra hydrogen source, which was determined to be the N–H of the amine additive. In another controlled experiment under D<sub>2</sub> with deuterium-labeled MPA (MPA-d<sub>1</sub>) the deuterium content at the 2-position of (S)-5a-d<sub>1</sub> increased to 87% (Scheme 7c), which indicated that the amine proton of MPA was involved in the catalytically active species as a hydride ligand to be transferred to the C=N double bond of 4a-1,2-H<sub>2</sub>. Even under the latter conditions, 13% of the proton at the 2-position of (S)-5a was not deuterated, most likely because 4a-1,2-H<sub>2</sub> also contains an amine proton.

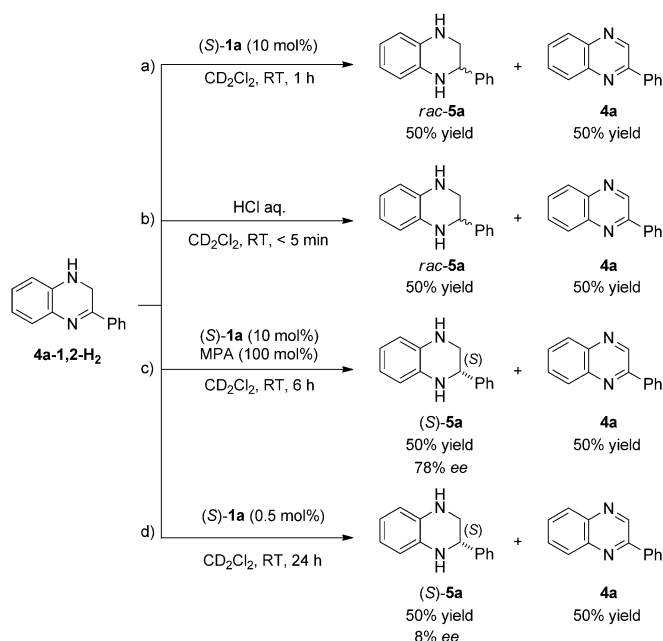
We conducted further controlled experiments with 4a-1,2-H<sub>2</sub> in the absence of H<sub>2</sub>, outlined in Scheme 8. Surprisingly, treatment of 4a-1,2-H<sub>2</sub> with (S)-1a (10 mol%) in CD<sub>2</sub>Cl<sub>2</sub> at room temperature spontaneously gave a 1:1 mixture of 4a and racemic 5a (Scheme 8a). A trace amount of acid derived from (S)-1a, which was synthesized by the addition of HCl to the Ir<sup>I</sup> precursor (see Experimental), catalyzed dis-

proportionation, evidenced by the fact that the same disproportionation<sup>[21]</sup> occurred when 4a-1,2-H<sub>2</sub> was treated with HCl (Scheme 8b). In contrast, treatment of 4a-1,2-H<sub>2</sub> with (S)-1a (10 mol%) in the presence of MPA (100 mol%) induced enantioselective disproportionation to give (S)-5a in 78% ee (Scheme 8c), although the reaction rate was slower (6 h) than that of racemic disproportionation,



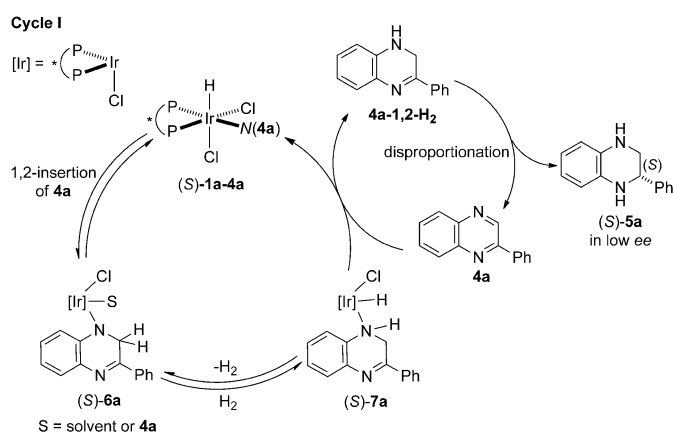
Scheme 7. Asymmetric hydrogenation and asymmetric deuteration of 4a-1,2-H<sub>2</sub> under various reaction conditions.

tion (<1 h). Notably, a small amount of (S)-1a (0.5 mol%) catalyzed the disproportionation of 4a-1,2-H<sub>2</sub> to give (S)-5a enantioselectively (8% ee), even in the absence of MPA (Scheme 8d), because the reduced product 5a has an amine moiety that functions as an amine additive to prevent the racemic disproportionation catalyzed by the acidic proton. <sup>1</sup>H NMR spectroscopy revealed that 4a-1,2-H<sub>2</sub> reacted with (S)-1a to generate an iridium–hydride species, which seemed to reduce 4a-1,2-H<sub>2</sub> to afford (S)-5a by asymmetric transfer hydrogenation from one molecule of 4a-1,2-H<sub>2</sub> to another. Some reduced N-heteroaromatic compounds are reported to function as transfer hydrogenation reagents; they easily generate hydrogen to reduce various unsaturated bonds.<sup>[3k,34,35]</sup> Thus, we concluded that the additional amine worked as a Brønsted base to capture acidic protons, which retarded the rapid racemic disproportionation of 4a-1,2-H<sub>2</sub> in catalytic cycle I.



Scheme 8. Disproportionation of **4a-1,2-H<sub>2</sub>** under various reaction conditions.

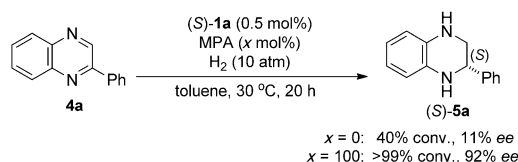
Based on these experimental outcomes, we propose the reduction mechanism of catalytic cycle I as shown in Scheme 9 and suggest that this mechanism plays a role in the catalytic cycle for the asymmetric hydrogenation of **4a** without any amine additives. The first step of cycle I was assumed to be a reversible 1,2-insertion of the C=N bond of **4a** into the Ir–H bond of (*S*)-**1a-4a** to give (*S*)-**6a**, followed by the addition of H<sub>2</sub> to the Ir–N bond to give (*S*)-**7a**, in which **4a-1,2-H<sub>2</sub>** is coordinated to the iridium center. Because **4a-1,2-H<sub>2</sub>** is spontaneously replaced by **4a**, (*S*)-**1a-4a** is regenerated under catalytic conditions. In principle, all of these steps, except for the replacement of **4a-1,2-H<sub>2</sub>** by **4a**, are reversible. The acidic proton derived from (*S*)-**1a** induces rapid racemic disproportionation of **4a-1,2-H<sub>2</sub>** (generat-



Scheme 9. Proposed mechanism of catalytic cycle I involving disproportionation of **4a-1,2-H<sub>2</sub>**.

ed in situ) to quinoxaline **4a** and tetrahydroquinoxaline **5a** and, at the same time, the chiral iridium complex might mediate slow the asymmetric disproportionation of **4a-1,2-H<sub>2</sub>** by asymmetric transfer hydrogenation, which might be mediated by the chiral iridium complex. Accordingly, in the absence of amine additive, the reduction of **4a** proceeded mainly by the rapid racemic disproportionation pathway to afford (*S*)-**5a** with low enantioselectivity. Accumulation of amine product **5a** as the reaction developed eliminated acidic impurities, thereby the involvement of the racemic pathway diminished (see below).

**Cycle II, catalyzed by (*S*)-1a-MPA:** In sharp contrast to the asymmetric hydrogenation of **4a** with (*S*)-**1a** under mild H<sub>2</sub> pressure (10 atm) without any amine additive to give (*S*)-**5a** in low conversion (40%) and low enantioselectivity (11% *ee*), the same reaction in the presence of adequate amounts of MPA (100 mol%) gave (*S*)-**5a** in full conversion with high enantioselectivity (92% *ee*; Scheme 10), which strongly indicated that the amine additive acted, not only as a Brønsted base to prevent racemic reduction, but also as an activator to improve catalytic activity under the hydrogenation conditions.



Scheme 10. Asymmetric hydrogenation of **4a** under mild H<sub>2</sub> pressure.

To reveal the activating effect of MPA under the hydrogenation conditions, we studied the controlled reaction of (*S*)-**1a** and H<sub>2</sub> gas in the presence and absence of MPA. Monitoring the <sup>1</sup>H NMR spectrum of the BINAP–Ir complex (*S*)-**1a** in CD<sub>2</sub>Cl<sub>2</sub> in the absence of MPA under exposure to atmospheric H<sub>2</sub> pressure for 20 h revealed no reaction. In sharp contrast, the addition of MPA (10 equiv) to (*S*)-**1a** in CD<sub>2</sub>Cl<sub>2</sub> dramatically changed the reaction under H<sub>2</sub> pressure (1 atm). After 30 min, we observed a new doublet of doublets centered at δ<sub>H</sub> = –13.8 ppm (*J*(H,P) = 16.6, 196.6 Hz) assigned to monohydride complex (*S*)-**8a** (Figure 5). The two *J*(H,P) coupling constants suggested that a hydride occupied the position *trans* to one phosphorus atom of the BINAP ligand of (*S*)-**8a** and *cis* to the other phosphorus atom, in sharp contrast to the general tendency that one hy-

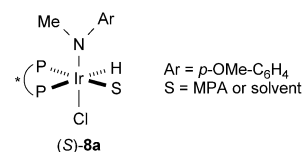


Figure 5. Tentative structure of transient monohydride species (*S*)-**8a**.

drude atom which is bound to iridium bearing a *cis*-chelating diphosphine ligand occupies the position *cis* to both phosphorous atoms of the chelating diphosphine ligand.<sup>[37]</sup> Because the hydride complex (*S*)-**8a** was a transient species that gradually decreased after 7 h and finally disappeared after 33 h, its isolation and characterization were hampered. However, (*S*)-**8a** was tentatively assigned as an amide-hydride species generated by the elimination of HCl from (*S*)-**1a-MPA** due to the quantitative formation of an MPA·HCl salt.<sup>[34]</sup>

As the reaction proceeded, we observed two sets of signals assigned to two trihydride dinuclear complexes, *anti*-(*S*)-**9a** and *syn*-(*S*)-**9a**, which appeared within 30 min and gradually increased in intensity (Figure 6). We successfully

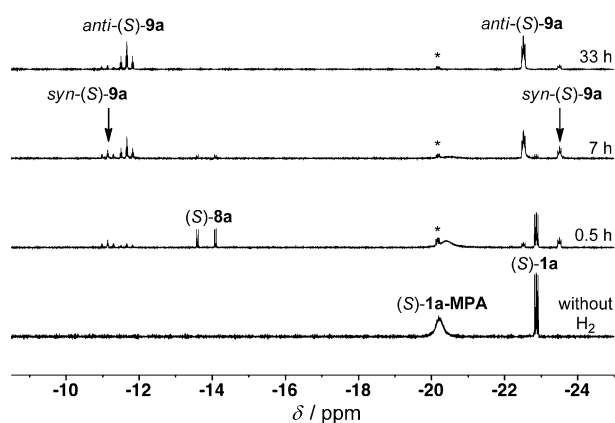
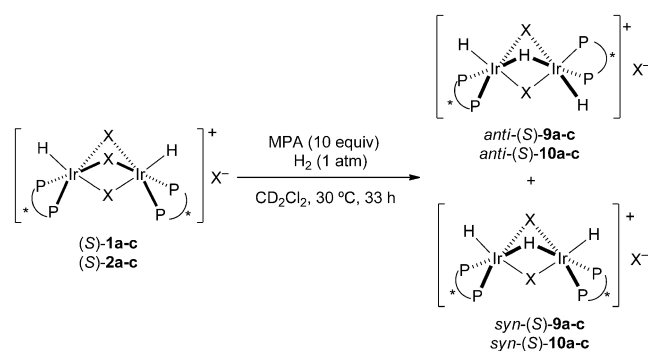


Figure 6. Time-dependent <sup>1</sup>H NMR spectra of hydride species in the reaction of (*S*)-**1a** and MPA (10 equiv) under H<sub>2</sub> (1 atm) at RT. Asterisk indicates an unidentified species.

isolated and characterized (by spectral measurements and X-ray crystal structural analysis) the trihydride dinuclear complex *anti*-(*S*)-**9a** and also its analogue *anti*-(*S*)-**10c**, which bears (*S*)-SEGPHOS and iodine ligands (Scheme 11). A pair of hydride signals centered at  $\delta_{\text{H}} = -11.1$  (tt,  $J(\text{H,H}) = 6.3$  Hz,  $J(\text{H,P}) = 63.0$  Hz; bridging hydride) and  $-23.4$  ppm (m; terminal hydride) in a 1:2 relative intensity were determined to be produced by *anti*-(*S*)-**9a**. Hydride signals of *syn*-(*S*)-**9a** were observed at  $\delta_{\text{H}} = -11.6$  (tt,  $J(\text{H,H}) = 8.5$  Hz,  $J(\text{H,P}) = 64.2$  Hz; bridging hydride) and



Scheme 11. Generation of trihydride dinuclear complexes.

$-22.4$  ppm (m; terminal hydride) with the same 1:2 relative intensity. Similar spectral data were obtained for *anti*-(*S*)-**10a-c** and *syn*-(*S*)-**10a-c**.<sup>[33]</sup> Mass spectral data for (*S*)-**9a** and (*S*)-**10c** confirmed that one of three bridging halide ligands was selectively replaced by one hydride ligand during the course of the reaction. Figure 7 shows the structure of *anti*-(*S*)-**10c**, in which two iridium centers are bridged by two iodide ligands and one hydride and, although the positions of three hydride moieties could not be located, each iridium center had a pseudo-octahedral and bifacial structure.

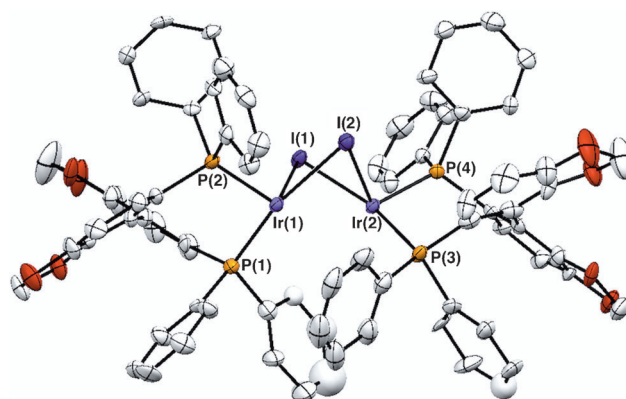
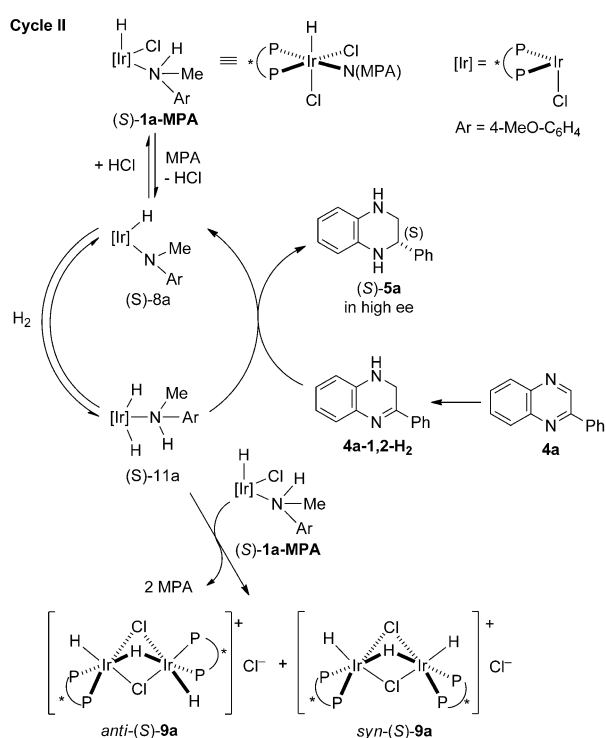


Figure 7. Crystal structure and numbering scheme of the cationic part of *anti*-(*S*)-**10c**. Selected bond lengths [Å] and angles [°]: Ir(1)–Ir(2) 2.845(5), Ir(1)–I(1) 2.781(7), Ir(1)–I(2) 2.751(7), Ir(2)–I(1) 2.744(6), Ir(2)–I(2) 2.800(7), Ir(1)–P(1) 2.263(3), Ir(1)–P(2) 2.285(2), Ir(2)–P(3) 2.247(3), Ir(2)–P(4) 2.278(3); P(1)–Ir(1)–P(2) 95.59(9), P(1)–Ir(1)–I(1) 97.43(7), P(1)–Ir(1)–I(2) 168.96(7), I(1)–Ir(1)–I(2) 82.92(2), P(2)–Ir(1)–I(2) 94.96(7), P(2)–Ir(1)–I(1) 105.16(7), P(3)–Ir(2)–P(4) 94.56(9), P(3)–Ir(2)–I(1) 167.43(7), P(3)–Ir(2)–I(2) 94.89(7), I(1)–Ir(2)–I(2) 82.70(2), P(4)–Ir(2)–I(1) 97.93(7), P(4)–Ir(2)–I(2) 107.22(7), Ir(1)–I(1)–Ir(2) 61.99(2), Ir(1)–I(2)–Ir(2) 61.66(2).

The mixture of *anti*- and *syn*-(*S*)-**9a** was determined to be catalytically inert because the isolated mixture showed no catalytic activity for the hydrogenation of **4a** under our standard reaction conditions (catalyst (0.5 mol %), H<sub>2</sub> (30 atm), 20 h, 30 °C). Notably, the presence of **4a** completely retarded the generation of (*S*)-**9a**, and reduction of **4a** to (*S*)-**5a** occurred preferentially.<sup>[33]</sup> Based on these results, (*S*)-**9a** was excluded from the catalytic cycle. In addition, the possibility of any dinuclear complex as a key intermediate in determining the enantioselectivity was ruled out because a nonlinear effect was not observed in the reaction; the enantiopurity of complex (*S*)-**1a** and the enantioselectivity of product (*S*)-**5a** had a linear relationship, indicative that a mononuclear species was the active species.<sup>[34]</sup>

These experimental outcomes led us to propose the reduction mechanism of catalytic cycle II, shown in Scheme 12. When the quantity of MPA was large enough, MPA coordinated to the iridium center to generate (*S*)-**1a-MPA**, even in the presence of strongly coordinating substrate **4a**. Elimination of HCl from (*S*)-**1a-MPA** afforded the amide-hydride species (*S*)-**8a**, which hydrogenated the



Scheme 12. Proposed mechanism of catalytic cycle II involving amide–hydride species (*S*)-**8a** and amine–dihydride species (*S*)-**11a**.

substrates **4a** and **4a-1,2-H<sub>2</sub>**. There are three possible mechanisms:

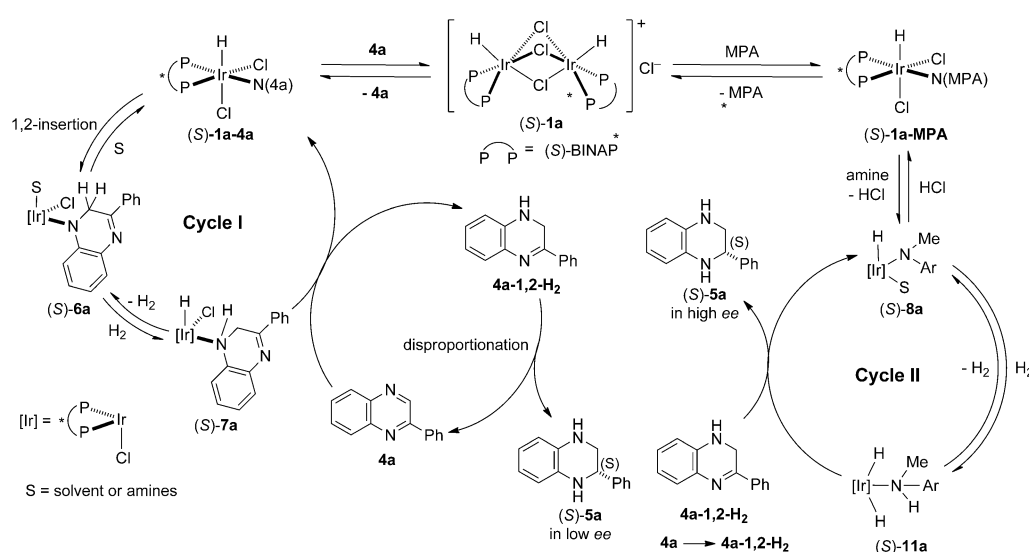
1) in the outer-sphere bifunctional mechanism, similar to Noyori's metal–amide bifunctional mechanism,<sup>[37]</sup> (*S*)-**8a** reacts with H<sub>2</sub> to form a highly catalytically active amine–dihydride species, (*S*)-**11a**, which hydrogenates **4a** and **4a-1,2-H<sub>2</sub>** to give the tetrahydrogenated product (*S*)-**5a**.

2) in the stepwise outer-sphere mechanism, a coordinating dihydrogen ligand is separated into proton and hydride to reduce the substrate by sequential proton-transfer and hydride-transfer reactions.<sup>[15]</sup>

3) in the inner-sphere mechanism, (*S*)-**8a** reacts with **4a** then **4a-1,2-H<sub>2</sub>** to give the product (*S*)-**5a** by 1,2-insertion of the substrate into the Ir–H bond, followed by heterolytic cleavage of H<sub>2</sub>.<sup>[27]</sup>

Although we could not definitely conclude which of the three mechanisms underlies the reaction, the formation of dinuclear trihydride complexes (*S*)-**9a** suggests the presence of amine–dihydride species (*S*)-**11a** (outer-sphere mechanism), in which the amine is labile and the nascent dihydride species might be trapped by (*S*)-**1a** or (*S*)-**1a-MPA** to give the dinuclear trihydride complexes (*S*)-**9a**. Furthermore, the assumed steric demand supports the outer-sphere mechanism because the inner-sphere mechanism requires unfavorable coordination of sterically hindered substrate **4a-1,2-H<sub>2</sub>** through its nitrogen atom.<sup>[33]</sup> In addition, our basic reaction conditions, which avoid racemic disproportionation, might exclude the stepwise outer-sphere reaction pathway, which involves protonation of substrates **4a** and **4a-1,2-H<sub>2</sub>**. Thus, MPA acted not only as a base to eliminate HCl by abstraction of one of two chloride atoms bound to the iridium center, but also as an amide ligand to generate a highly reactive and enantioselective catalytically active species. Although the iridium-catalyzed enantioselective disproportionation of **4a-1,2-H<sub>2</sub>** might occur in cycle II, the disproportionation is slow enough to be ignored (see Scheme 8 above).

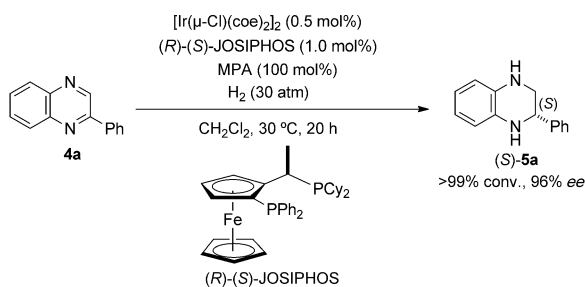
**Proposed entire reaction mechanism:** Based on the results of all of the controlled experiments described above, we postulate the complete catalytic cycle for the asymmetric hydrogenation of **4a** with (*S*)-**1a** as shown in Scheme 13, which comprises pre-equilibrium among (*S*)-**1a**, **4a**, and MPA, and



Scheme 13. Proposed complete catalytic cycle for the asymmetric hydrogenation of **4a**.

catalytic cycles I and II (the details of which are discussed above). Thus, the key events are the reversible coordination of substrate **4a** (cycle I) and MPA (cycle II) to the iridium dinuclear complex (*S*)-**1a** to give the corresponding mononuclear complexes (*S*)-**1a-4a** (cycle I) and (*S*)-**1a-MPA** (cycle II). Acidic protons derived from (*S*)-**1a** induce the fast disproportionation of **4a-1,2-H<sub>2</sub>** to **4a** and racemic **5a**; at the same time, the iridium complex (*S*)-**1a** induces slow asymmetric disproportionation to afford (*S*)-**5a**, resulting in low enantioselectivity at an early stage of the hydrogenation. As the amount of product amine **5a** increases, the acid-dependent disproportionation is suppressed. In the presence of excess amounts of MPA amide-hydrate Ir<sup>III</sup> species (*S*)-**8a** might be in equilibrium with (*S*)-**1a-MPA**, accompanied by dissociation of the HCl salt of MPA. The Ir–N bond of (*S*)-**8a** reversibly reacts with H<sub>2</sub> to give an amine-dihydrate species (*S*)-**11a**, which efficiently catalyzes the asymmetric hydrogenation of the C=N bond of **4a-1,2-H<sub>2</sub>** to give (*S*)-**5a** with high enantioselectivity (as well as the analogous reaction of **4a** to give **4a-1,2-H<sub>2</sub>**) through the bifunctional outer-sphere mechanism. At this stage, acid-catalyzed racemic disproportionation is strongly inhibited by amines present in the reaction mixture.

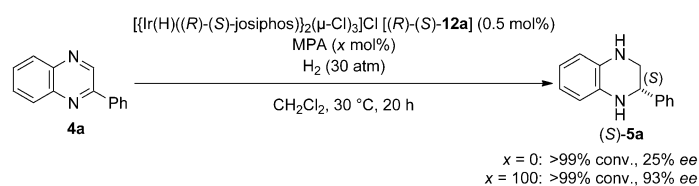
**Direct generation of amide species:** In the asymmetric hydrogenation of imines, quinolines, and quinoxalines catalyzed by chiral iridium complexes, iodine is usually used as an additive for the oxidation of an Ir<sup>I</sup> precursor<sup>[31]</sup> (e.g. [IrX(olefin)<sub>2</sub>]/chiral chelating diphosphine ligand) to give a catalyst system that involves an Ir<sup>III</sup> species. As revealed in the above sections, the formation of Ir<sup>III</sup>–amide species proceeded in the reaction of Ir<sup>III</sup> halide complexes with amines. Therefore, we used MPA as a reagent to generate an Ir<sup>III</sup>–amide species by oxidative addition of the N–H bond to Ir<sup>I</sup>, but the direct reaction of Ir<sup>I</sup> supported by BINAP, SEGPHOS, and DIFLUORPHOS ligands did not produce any products identifiable by NMR spectroscopy. We then focused on the JOSIPHOS ligand (Scheme 14), the Ir<sup>I</sup> complex of which is reported to act as a catalyst for asymmetric hydroamination of C=C double bonds by aniline derivatives to.<sup>[38]</sup> In the case of iridium-catalyzed hydroamination, a monomeric neutral amide-hydrate Ir<sup>III</sup> species is the active catalyst.<sup>[39]</sup> Unexpectedly, the addition of MPA to [IrCl(coe)<sub>2</sub>]<sub>2</sub> (coe = cyclooctene) in the presence of (*R*)-(*S*)-JOSIPHOS



Scheme 14. Asymmetric hydrogenation of **4a** catalyzed by Ir<sup>I</sup>-Josiphos/MPA system.

PHOS became the superior catalyst for asymmetric hydrogenation of **4a** under standard reaction conditions to give (*S*)-**5a** with a 96% *ee* (Scheme 14). This result is consistent with our proposed mechanism because the Ir<sup>I</sup>–JOSIPHOS/MPA system directly generates a highly catalytically active mononuclear amide-hydrate Ir<sup>III</sup> species analogous to (*S*)-**8a**. The advantages of this system are: 1) no HCl elimination process, which eliminates hydrogen chloride mediated racemic disproportionation of the half-reduced product **4a-1,2-H<sub>2</sub>**, and 2) no retro reaction of the amide-hydrate complex analogous to (*S*)-**8a** to form a bis-chloride amine-hydrate complex analogous to (*S*)-**1a-MPA**. Thus, under such a catalytic system, only cycle II, which involves a highly active amide-hydrate species, spontaneously proceeded.

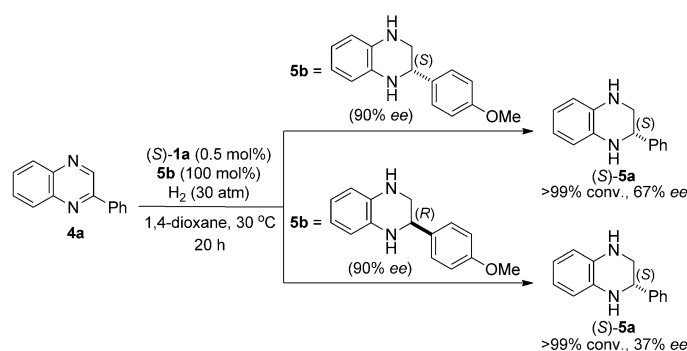
In addition, we successfully synthesized a chloride-bridged iridium dinuclear complex [(*R*)-(*S*)-**12a**], with a coordinated (*R*)-(*S*)-JOSIPHOS ligand, to confirm its catalytic activity in the asymmetric hydrogenation of **4a** with (100 mol%) or without MPA. In absence of MPA, 25% *ee* was realized, whereas the addition of MPA drastically increased the enantioselectivity to 93% *ee* (Scheme 15). These results suggested that the hydrogenation catalyzed by the (*R*)-(*S*)-JOSIPHOS complex (*R*)-(*S*)-**12a** proceeded through the same reaction mechanism as that catalyzed by (*S*)-**1a**, which involved a disproportionation of **4a-1,2-H<sub>2</sub>**.



Scheme 15. Asymmetric hydrogenation of **4a** catalyzed by (*R*)-(*S*)-**12a**.

**Positive feedback from the product amine:** Large amounts of amine in the reaction mixture improved, not only the catalytic activity, but also the enantioselectivity, therefore, we anticipated that hydrogenated product **5a** would show similar additive effects to generate the highly active amide-hydrate species described in Scheme 13. Addition of (*S*)-4-methoxyphenyl-1,2,3,4-tetrahydroquinoxaline [(*S*)-**5b**] (100 mol%, 90% *ee*) or (*R*)-**5b** (100 mol%, 90% *ee*) to the reagents for asymmetric hydrogenation of **4a** with (*S*)-**1a** efficiently increased or decreased the enantioselectivity of (*S*)-**5a**, respectively, dependent on the match or mismatch of the stereochemistry to the chiral ligand of (*S*)-**1a** and the chiral product **5b** (Scheme 16). This match-and-mismatch effect observed for the asymmetric hydrogenation of **4a** strongly suggested that the diastereomeric amine-hydrate complex was a key intermediate.

Encouraged by our observations, we added product **5a** to subsequent hydrogenation reactions of **4a**. Thus, the first asymmetric hydrogenation of **4a** under H<sub>2</sub> (30 atm) at 30 °C for 20 h in 1,4-dioxane with (*S*)-**1a** (0.5 mol%) gave (*S*)-**5a** in moderate *ee* (59%). The time dependence of the conver-



Scheme 16. Additive effect of chiral product **5b** and match-and-mismatch effect.

sion of **4a** and *ee* of (*S*)-**5a** (Figure 8a) plotted at 1, 3, 5, and 7 h revealed that the yield of (*S*)-**5a** increased exponentially over time, alongside a dramatic increase in enantioselectivity. Surprisingly, the second reduction of **4a** with (*S*)-**1a** in the presence of (*S*)-**5a** (100 mol%, 59% *ee*)—the product of the first asymmetric hydrogenation—afforded (*S*)-**5a** with an enriched *ee* (65%); the net enantioselectivity of the second hydrogenation of **4a** was estimated to be 72% *ee*. We conducted a third asymmetric hydrogenation of **4a** with (*S*)-**1a** in the presence of (*S*)-**5a** (100 mol%, 65% *ee*) and the reduction afforded (*S*)-**5a** with 70% *ee* (the net enantioselectivity of the third reaction was estimated to be 75% *ee*; Figure 8b). This observation was consistent with the mechanism outlined in Scheme 13 above. The same enhancement phenomenon was observed for the reduction of **4a** with SEGPHOS complex (*S*)-**2a** under the same reaction conditions. Thus, we demonstrated positive feedback of the product amine. Such enhanced positive feedback to metal-assisted asymmetric reactions by a chiral product was first reported by Soai (asymmetric autocatalysis),<sup>[40]</sup> the addition of diisopropylzinc to pyrimidine-5-car-

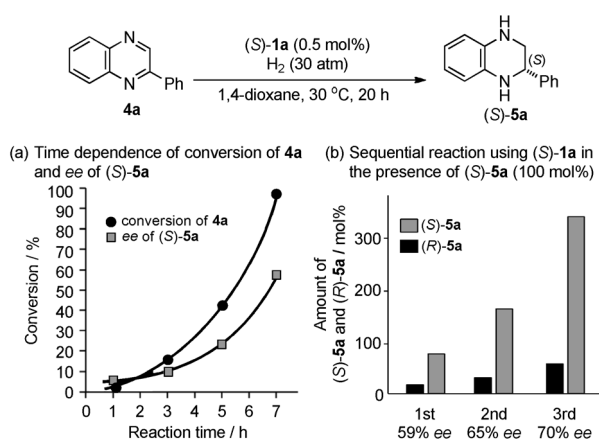


Figure 8. a) Time course for the conversion of **4a** (●) and enantiomeric excess of (*S*)-**5a** (■) in the asymmetric hydrogenation of **4a** catalyzed by Ir complex (*S*)-**1a**. b) Sequential reaction catalyzed by (*S*)-**1a** in the presence of enantioenriched (*S*)-**5a** (100 mol%) obtained from the previous reaction (■ = (*S*)-**5a**; ■ = (*R*)-**5a**).

boxaldehyde was catalyzed by the addition of slightly enantiomeric enriched 2-methyl-1-(5-pyrimidyl)propan-1-ol, which operated as the ligand of the zinc catalyst to give highly enantiomerically enriched 2-methyl-1-(5-pyrimidyl)propan-1-ol upon hydrolysis, but, to the best of our knowledge, our iridium catalyst system is the first example of a transition-metal-catalyzed system.

## Conclusion

We report the mild asymmetric hydrogenation of quinoxalines catalyzed by chiral dinuclear triply halide-bridged iridium complexes. An amine additive not only enhanced catalytic activity but also the enantioselectivity. Our air-stable precursors allow the reaction to be performed without exhaustive purification or special handling. Mechanistic studies indicated a dual mechanism that involved two individual catalytic cycles in equilibrium. Each of the proposed intermediates in our catalytic cycle was either isolated or spectroscopically characterized and a series of stoichiometric reactions confirmed their role in the catalytic cycle. The key species was amide-hydride species **8a**, which demonstrated high catalytic activity and hydrogenated substrate **4a** to give product **5a** with high enantioselectivity. Based on the proposed mechanism, the highest selectivity was achieved by using the JOSIPHOS ligand. In addition, we revealed that hydrogenated product **5a** had similar additive effects, as well as positive-feedback enhancement, in which the presence of a partially enantiomerically enriched hydrogenated product **5a** improved both the reaction rate and enantioselectivity upon use in subsequent asymmetric reductions of **4a**. This is the first report of positive-feedback enhancement in asymmetric hydrogenation, rationalized by the proposed dual mechanism. The new catalyst system of a halo-Ir<sup>III</sup> precursor combined with large amounts of amine clearly shows the important role of the amine, not only as a ligand to generate the highly reactive and enantioselective iridium-amide species, but also as a Brønsted base to bypass the acid-catalyzed racemic disproportionation of half-reduced compound **4a-1,2-H<sub>2</sub>** in the iridium-catalyzed asymmetric hydrogenation of **4a**. Our results could lead to the development of asymmetric hydrogenation of N-heteroaromatic compounds and other C=N bonds under mild conditions. Further extension of this new catalyst system is ongoing.

## Experimental Section

**General procedure for asymmetric hydrogenation of 2-arylquinoxalines (4):** A glass tube was charged with **4** (0.42 mmol), iridium complex (2.1 μmol, 0.5 mol%), and amine additive (110 mol%) if required. The glass tube was placed in an autoclave. After three cycles of evacuation/argon backfilling, solvent (3.0 mL) was added from the inlet, the mixture was charged with H<sub>2</sub>, then the hydrogen pressure was increased (30 atm). The reaction mixture was stirred at 30 °C for the indicated time. After release of H<sub>2</sub>, the solvent was removed by evaporation. The conversion and *ee* were determined by <sup>1</sup>H NMR spectroscopy and HPLC

analysis of the crude product. The product was purified by filtration through a short pad of silica gel (8:2 hexane/EtOAc), and analyzed by spectroscopic methods.

**Complex (S)-1a-PA:** A mixture of (S)-1a (13 mg, 7.3  $\mu$ mol) and *p*-methoxyaniline (2.1 equiv, 1.9 mg, 15.3  $\mu$ mol) in CH<sub>2</sub>Cl<sub>2</sub> (0.6 mL) was stirred for 1 h at RT to give a pale-brown solution. Addition of hexane afforded (S)-1a-PA as a pink powder, which was recrystallized from Et<sub>2</sub>O/CH<sub>2</sub>Cl<sub>2</sub>. M.p. 120–130 °C (decomp.); <sup>1</sup>H NMR (400 MHz, CD<sub>2</sub>Cl<sub>2</sub>, 30 °C):  $\delta$  = 8.1–7.2 (m, 20H; Ar), 7.0–6.2 (m, 16H; Ar), 3.6 (s, 3H; MeO), –20.1 ppm (dd, *J*(H,P) = 14.2, 21.4 Hz, 1H; Ir-H); <sup>31</sup>P NMR (161 MHz, CD<sub>2</sub>Cl<sub>2</sub>, 30 °C):  $\delta$  = 0.3 (d, *J*(P,P) = 18.6 Hz), –5.6 ppm (d, *J*(P,P) = 18.6 Hz); ESI-MS (MeOH, 180 °C, 4.5 kV): *m/z*: calcd: 1008.17 [M–H]<sup>+</sup>; found: 1008.15; elemental analysis calcd (%) for C<sub>51</sub>H<sub>42</sub>Cl<sub>2</sub>IrNOP<sub>2</sub>: C 60.65, H 4.19, N 1.39; found: C 60.95, H 3.72, N, 1.51.

**Complex (S)-2a-PA:** The title complex was synthesized from (S)-2a as described for (S)-1a-PA above. M.p. 153–162 °C (decomp.); <sup>1</sup>H NMR (400 MHz, CD<sub>2</sub>Cl<sub>2</sub>, 30 °C):  $\delta$  = 7.9–7.1 (m, 20H; Ar), 6.5–5.7 (m, 8H; Ar), 5.3 (m, 4H; OCH<sub>2</sub>O), 4.4 (brs, 2H; NH<sub>2</sub>), 3.7 (s, 3H; MeO), –20.1 ppm (dd, *J*(H,P) = 13.9, 21.4 Hz, 1H; Ir-H); <sup>31</sup>P NMR (161 MHz, CD<sub>2</sub>Cl<sub>2</sub>, 30 °C):  $\delta$  = –0.8 (d, *J*(P,P) = 19.2 Hz), –7.2 ppm (d, *J*(P,P) = 19.2 Hz); ESI-MS (MeOH, 180 °C, 4.5 kV): *m/z*: calcd: 996.10 [M–H]<sup>+</sup>; found: 996.11; elemental analysis calcd (%) for C<sub>45</sub>H<sub>38</sub>Cl<sub>2</sub>IrNO<sub>3</sub>P<sub>2</sub>·CH<sub>2</sub>Cl<sub>2</sub>: C 51.02, H 3.72, N, 1.29; found: C 50.86, H 3.57, N, 1.28.

**Complex (S)-9a:** A brown solution of (S)-1a (50 mg, 28  $\mu$ mol) and MPA (10 equiv, 39 mg, 0.28 mmol) in CH<sub>2</sub>Cl<sub>2</sub> (1.0 mL) was exposed to atmospheric pressure of H<sub>2</sub> and stirred vigorously for 48 h. Addition of hexane afforded *anti*-(S)-9a as yellow powder, which was recrystallized from Et<sub>2</sub>O/CH<sub>2</sub>Cl<sub>2</sub>.

**Complex *anti*-(S)-9a (thermodynamic product):** M.p. 175–185 °C (decomp.); <sup>1</sup>H NMR (400 MHz, CD<sub>2</sub>Cl<sub>2</sub>, 30 °C):  $\delta$  = 7.9–7.3 (m, 40H; PPh<sub>2</sub>), 7.1–6.5 (m, 24H; Ar), –11.6 (tt, *J*(H,H) = 8.5 Hz, *J*(H,P) = 64.2 Hz, 1H;  $\mu$ -H), –22.4 ppm (m, 2H; Ir-H); <sup>31</sup>P NMR (161 MHz, CD<sub>2</sub>Cl<sub>2</sub>, 30 °C):  $\delta$  = 5.0 (br), 3.2 ppm (br); ESI-MS (MeOH, 180 °C, 4.5 kV): *m/z*: calcd: 1703.28 [M–Cl]<sup>+</sup>; found: 1703.28; elemental analysis calcd (%) for C<sub>88</sub>H<sub>67</sub>Cl<sub>3</sub>Ir<sub>2</sub>P<sub>4</sub>·2CH<sub>2</sub>Cl<sub>2</sub>: C 56.62, H 3.75; found: C 56.76, H 3.28.

**Complex *syn*-(S)-9a (kinetic product):** This complex could not be isolated. The aromatic proton signals are not described because the region was observed as multiplet peak that overlapped with signals from *anti*-(S)-9a and MPA. <sup>1</sup>H NMR (400 MHz, CD<sub>2</sub>Cl<sub>2</sub>, 30 °C):  $\delta$  = –11.1 (tt, *J*(H,H) = 6.3 Hz, *J*(H,P) = 63.0 Hz, 1H;  $\mu$ -H), –23.4 ppm (m, 2H; Ir-H); <sup>31</sup>P NMR (161 MHz, CD<sub>2</sub>Cl<sub>2</sub>, 30 °C):  $\delta$  = 6.0 (br), 2.0 ppm (br).

**Complex (S)-10c:** The title complex was synthesized and purified as described above for (S)-9a.

**Complex *anti*-(S)-10c (thermodynamic product):** <sup>1</sup>H NMR (400 MHz, CD<sub>2</sub>Cl<sub>2</sub>, 30 °C):  $\delta$  = 7.5–7.1 (m, 40H; Ar), 6.6 (dd, *J*(H,H) = 1.7, 8.2 Hz, 2H; Ar), 6.2 (d, *J*(H,H) = 8.2 Hz, 2H; Ar), 6.0 (m, 2H), 5.8 (dd, *J*(H,H) = 1.3, 41.1 Hz, 4H; OCH<sub>2</sub>O), 5.6 (dd, *J*(H,H) = 8.2, 24.7 Hz, 4H; OCH<sub>2</sub>O), 5.2 (m, 2H) –13.5 (tt, *J*(H,H) = 9.0 Hz, *J*(H,P) = 57.6 Hz, 1H;  $\mu$ -H), –19.0 ppm (m, 2H; Ir-H); <sup>31</sup>P NMR (161 MHz, CD<sub>2</sub>Cl<sub>2</sub>, 30 °C):  $\delta$  = –4.1 (br), –5.1 ppm (t, *J*(P,P) = 8.5 Hz); ESI-MS (MeOH, 180 °C, 4.5 kV): *m/z*: calcd: 1863.05 [M–I]<sup>+</sup>; found: 1863.06; elemental analysis calcd (%) for C<sub>76</sub>H<sub>59</sub>I<sub>3</sub>Ir<sub>2</sub>O<sub>8</sub>P<sub>4</sub>·3CH<sub>2</sub>Cl<sub>2</sub>: C 42.28, H 2.92; found: C 42.41, H 2.23.

**Complex *syn*-(S)-10c (kinetic product):** This complex could not be isolated. Aromatic proton region is not described because the region was observed as multiplet peak overlapped with *anti*-(S)-10c and MPA in the reaction mixture. <sup>1</sup>H NMR (400 MHz, CD<sub>2</sub>Cl<sub>2</sub>, 30 °C):  $\delta$  = –13.6 (tt, *J*(H,H) = 5.2 Hz, *J*(H,P) = 56.5 Hz, 1H;  $\mu$ -H), –20.6 ppm (m, 2H; Ir-H); <sup>31</sup>P NMR (161 MHz, CD<sub>2</sub>Cl<sub>2</sub>, 30 °C):  $\delta$  = –10.9 (br), –12.2 ppm (br).

## Acknowledgements

This work was supported by the Core Research for Evolutional Science and Technology (CREST) Program of the Japan Science and Technology Agency (JST), Japan. We thank Prof. J.-P. Genêt, Dr. V. Ratovelomana-

na-Vidal, and Dr. T. Ayad (ENSCP, France) for their discussions regarding the asymmetric hydrogenation of quinoxalines. T.N. expresses his special thanks for the financial support provided by the JSPS Research Fellowships for Young Scientists. A.I. appreciates the financial support supplied by the Institutional Program for Young Researcher Overseas Visits (JSPS) for his stay in ETH Zürich.

- [1] a) R. Noyori, *Asymmetric Catalysis in Organic Synthesis*, Wiley, New York, **1994**, Chapter 2, pp. 16–94; b) J. M. Brown, R. L. Halterman, T. Ohkuma, R. Noyori, H.-U. Blaser, F. Spindler in *Comprehensive Asymmetric Catalysis, Vol. 1* (Eds.: E. N. Jacobsen, A. Pfaltz, H. Yamamoto), Springer, Berlin, **1999**, pp. 122–266; c) S. J. Roseblade, A. Pfaltz, *Acc. Chem. Res.* **2007**, *40*, 1402–1411; d) G. Shang, W. Li, X. Zhang in *Catalytic Asymmetric Synthesis*, 3rd ed. (Ed.: I. Ojima), Wiley, Hoboken, **2010**, Chapter 7, pp. 343–436; e) D. J. Ager, C. J. Cobley, P. H. Moran, H.-U. Blaser, M. Lotz, F. Spindler, Y. Chi, W. Tang, X. Zhang, S. H. L. Kok, T. T.-L. Au-Yeung, H. Y. Cheung, W. S. Lam, S. S. Chan, A. S. C. Chan, M. van den Berg, B. L. Feringa, A. J. Minnaard, A. Pfaltz, S. Bell, J. M. Brown, T. Ohkuma, R. Noyori, A. Mortreux, A. Karim, A. J. Blacker, J. G. de Vries, L. Lefort, M. Thommen in *Handbook of Homogeneous Hydrogenation*, (Eds.: J. G. de Vries, C. J. Elsevier), Wiley-VCH, Weinheim, **2007**, Part 4, pp. 745–1324; f) K. Püntener, M. Scalone, W. Bonrath, R. Karge, T. Netcher, F. Roessler, F. Spindler in *Asymmetric Catalysis on Industrial Scale: Challenges, Approaches and Solutions*, 2nd ed. (Eds.: H. U. Blaser, H. J. Federsel), Wiley-VCH, Weinheim, **2010**, Chapters 2 and 3, pp. 13–38.
- [2] For reviews, see: a) Y.-G. Zhou, *Acc. Chem. Res.* **2007**, *40*, 1357–1366; b) D.-S. Wang, Q.-A. Chen, S.-M. Lu, Y.-G. Zhou, *Chem. Rev.* **2012**, *112*, 2557–2590.
- [3] a) W.-B. Wang, S.-M. Lu, P. Y. Yang, X.-W. Han, Y.-G. Zhou, *J. Am. Chem. Soc.* **2003**, *125*, 10536–10537; b) S.-M. Lu, X.-W. Han, Y.-G. Zhou, *Adv. Synth. Catal.* **2004**, *346*, 909–912; c) S.-M. Lu, Y.-Q. Wang, X.-W. Han, Y.-G. Zhou, *Angew. Chem.* **2006**, *118*, 2318–2321; *Angew. Chem. Int. Ed.* **2006**, *45*, 2260–2263; d) W.-J. Tang, S.-F. Zhu, L.-J. Xu, Q.-L. Zhou, Q.-H. Fan, H.-F. Zhou, K. Lam, A. S. C. Chan, *Chem. Commun.* **2007**, 613–615; e) X.-B. Wang, Y.-G. Zhou, *J. Org. Chem.* **2008**, *73*, 5640–5642; f) D.-W.; Wang, D.-S. Wang, Q.-A. Chen, Y.-G. Zhou, *Chem. Eur. J.* **2010**, *16*, 1133–1136; Wang, X.-B. Wang, D.-S. Wang, S.-M. Lu, Y.-G. Zhou, Y.-X. Li, *J. Org. Chem.* **2009**, *74*, 2780–2787; g) D.-S. Wang, J. Zhou, D.-W. Wang, Y.-L. Guo, Y.-G. Zhou, *Tetrahedron Lett.* **2010**, *51*, 525–528; h) W. Tang, Y. Sun, L. Xu, T. Wang, Q. Fan, K.-H. Lam, A. S. C. Chan, *Org. Biomol. Chem.* **2010**, *8*, 3464–3471; i) D.-S. Wang, Y.-G. Zhou, *Tetrahedron Lett.* **2010**, *51*, 3014–3017; j) D.-Y. Zhang, D.-S. Wang, M.-C. Wang, C.-B. Yu, K. Gao, Y.-G. Zhou, *Synthesis* **2011**, 2796–2802; k) Q.-A. Chen, K. Gao, Y. Duan, Z.-S. Ye, Y. Yang, Y.-G. Zhou, *J. Am. Chem. Soc.* **2012**, *134*, 2442–2448; l) D.-W.; Wang, D.-S. Wang, Q.-A. Chen, Y.-G. Zhou, *Chem. Eur. J.* **2010**, *16*, 1133–1136.
- [4] a) L. Xu, K. H. Lam, J. Li, J. Wu, Q.-H. Fan, W.-H. Lo, A. S. C. Chan, *Chem. Commun.* **2005**, 1390–1392; b) K. H. Lam, L. Xu, L. Feng, Q.-H. Fan, F. L. Lam, W.-H. Lo, A. S. C. Chan, *Adv. Synth. Catal.* **2005**, *347*, 1755–1758; c) L. Qiu, F. Y. Kwong, J. Wu, W. H. Lam, S. Chan, W.-Y. Yu, Y.-M. Li, R. Guo, Z. Zhou, A. S. C. Chan, *J. Am. Chem. Soc.* **2006**, *128*, 5955–5965; d) S. H. Chan, K. H. Lam, Y.-M. Li, L. Xu, W. Tang, F. L. Lam, W. H. Lo, W. Y. Yiu, Q. Fan, A. S. C. Chan, *Tetrahedron: Asymmetry* **2007**, *18*, 2625–2631; e) H. Zhou, Z. Li, Z. Wang, T. Wang, L. Xu, Y. He, Q.-H. Fan, J. Pan, L. Gu, A. S. C. Chan, *Angew. Chem.* **2008**, *120*, 8592–8595; *Angew. Chem. Int. Ed.* **2008**, *47*, 8464–8467; f) W. Tang, L. Xu, Q.-H. Fan, J. Wang, B. Fan, Z. Zhou, K. H. Lam, A. S. C. Chan, *Angew. Chem.* **2009**, *121*, 9299–9302; *Angew. Chem. Int. Ed.* **2009**, *48*, 9135–9138; g) W.-J. Tang, J. Tan, L.-J. Xu, K. H. Lam, Q.-H. Fan, A. S. C. Chan, *Adv. Synth. Catal.* **2010**, *352*, 1055–1062; h) T. Wang, L.-G. Zhuo, Z. Li, F. Chen, Z. Ding, Y. He, Q.-H. Fan, J. Xiang, Z.-X. Yu, A. S. C. Chan, *J. Am. Chem. Soc.* **2011**, *133*, 9878–9891.
- [5] a) Z.-J. Wang, G.-J. Deng, Y. Li, Y.-M. He, W.-J. Tang, Q.-H. Fan, *Org. Lett.* **2007**, *9*, 1243–1246; b) Z.-J. Wang, H.-F. Zhou, T.-L.

- Wang, Y.-M. He, Q.-H. Fan, *Green Chem.* **2009**, *11*, 767–769; c) Z.-W. Li, T.-L. Wang, Y.-M. He, Z.-J. Wang, Q.-H. Fan, J. Pan, L.-J. Xu, *Org. Lett.* **2008**, *10*, 5265–5268; d) T. Wang, G. Ouyang, Y.-M. He, Q.-H. Fan, *Synlett* **2011**, 939–942.
- [6] a) C. Deport, M. Buchotte, K. Abecassis, H. Tadaoka, T. Ayad, T. Ohshima, J.-P. Genêt, K. Mashima, V. Ratovelomanana-Vidal, *Synlett* **2007**, 2743–2747; b) H. Tadaoka, D. Cartigny, T. Nagano, T. Gosavi, T. Ayad, J.-P. Genêt, T. Ohshima, V. Ratovelomanana-Vidal, K. Mashima, *Chem. Eur. J.* **2009**, *15*, 9990–9994.
- [7] M. T. Reetz, X. Li, *Chem. Commun.* **2006**, 2159–2160.
- [8] N. Mršić, L. Lefort, B. Laurent, A. F. Jeroen, A. J. Minnaard, B. L. Feringa, J. G. de Vries, *Adv. Synth. Catal.* **2008**, *350*, 1081–1089.
- [9] S.-M. Lu, C. Bolm, *Adv. Synth. Catal.* **2008**, *350*, 1101–1105.
- [10] M. Eggenstein, A. Thomas, J. Theuerkauf, G. Francio, W. Leitner, *Adv. Synth. Catal.* **2009**, *351*, 725–732.
- [11] F.-R. Gou, W. Li, X. Zhang, Y.-M. Liang, *Adv. Synth. Catal.* **2010**, *352*, 2441–2444.
- [12] M. Rubio, A. Pizzano, *Molecules* **2010**, *15*, 7732–7741.
- [13] J. L. Núñez-Rico, H.-F. Fernández-Pérez, J. Benet-Buchholz, A. Vidal-Ferran, *Organometallics* **2010**, *29*, 6627–6631.
- [14] M. Rueping, R. M. Koenigs, *Chem. Commun.* **2011**, 47, 304–306.
- [15] G. E. Dobreiner, A. Nova, N. D. Schley, N. Hazari, S. J. Miller, O. Eisenstein, R. H. Crabtree, *J. Am. Chem. Soc.* **2011**, *133*, 7547–7562.
- [16] S. Murata, T. Sugimoto, S. Matsuura, *Heterocycles* **1987**, *26*, 763–766.
- [17] a) C. Bianchini, P. Barbaro, G. Scapacci, E. Farnetti, M. Graziani, *Organometallics* **1998**, *17*, 3308–3310; b) C. Bianchini, P. Barbaro, G. Scapacci, *J. Organomet. Chem.* **2001**, *621*, 26–33.
- [18] a) C. J. Cobley, J. P. Henschke, *Adv. Synth. Catal.* **2003**, *345*, 195–201; b) J. P. Henschke, M. J. Burk, C. G. Malan, D. Herzberg, J. A. Peterson, A. J. Wildsmith, C. J. Cobley, G. Casy, *Adv. Synth. Catal.* **2003**, *345*, 300–307.
- [19] N. Mršić, T. Jerphagnon, A. Minnaard, B. L. Feringa, J. de Vries, *Adv. Synth. Catal.* **2009**, *351*, 2549–2552.
- [20] a) D. Cartigny, T. Nagano, T. Ayad, J.-P. Genêt, T. Ohshima, K. Mashima, V. Ratovelomanana-Vidal, *Adv. Synth. Catal.* **2010**, *352*, 1886–1891; b) D. Cartigny, F. Berhal, T. Nagano, P. Phansavath, T. Ayad, J.-P. Genêt, T. Ohshima, K. Mashima, V. Ratovelomanana-Vidal, *J. Org. Chem.* **2012**, *77*, 4544–4556.
- [21] Q.-A. Chen, D.-S. Wang, Y.-G. Zhou, Y. Duan, H.-J. Fan, Y. Yang, Z. Zhang, *J. Am. Chem. Soc.* **2011**, *133*, 6126–6129.
- [22] J. Qin, Z. Ding, Y.-M. He, L. Xu, Q.-H. Fan, *Org. Lett.* **2011**, *13*, 6568–6571.
- [23] a) M. Studer, C. Wedemeyer-Exl, F. Spindler, H. U. Blaser, *Monatsh. Chem.* **2000**, *131*, 1335–1343; b) L. Hegedüs, V. Hada, A. Tungler, T. Máthé, L. Szepesy, *Appl. Catal. A* **2000**, *201*, 107–114; c) N. Douja, M. Besson, P. Gallezot, C. Pinel, *J. Mol. Catal. A Chem.* **2002**, *186*, 145–151; d) N. Douja, R. Malacea, M. Banciu, M. Besson, C. Pinel, *Tetrahedron Lett.* **2003**, *44*, 6991–6993; e) F. Glorius, N. Spielkamp, S. Holle, R. Goddard, C. W. Lehmann, *Angew. Chem.* **2004**, *116*, 2910–2913; *Angew. Chem. Int. Ed.* **2004**, *43*, 2850–2852; f) C. Y. Legault, A. B. Charette, *J. Am. Chem. Soc.* **2005**, *127*, 8966–8967; g) A. W. Lei, M. Chen, M. S. He, X. Zhang, *Eur. J. Org. Chem.* **2006**, 4343–4347; h) X.-B. Wang, W. Zeng, Y.-G. Zhou, *Tetrahedron Lett.* **2008**, *49*, 4922–4924.
- [24] a) R. Kuwano, M. Kashiwabara, M. Ohsumi, H. Kusano, *J. Am. Chem. Soc.* **2007**, *129*, 3802; b) R. Kuwano, *Heterocycles* **2008**, *76*, 909–922; c) D.-S. Wang, Z.-S. Ye, Q.-A. Chen, Y.-G. Zhou, C.-B. Yu, H.-J. Fan, Y. Duan, *J. Am. Chem. Soc.* **2011**, *133*, 8866–8869.
- [25] R. Kuwano, N. Kameyama, R. Ikeda, *J. Am. Chem. Soc.* **2011**, *133*, 7312–7315.
- [26] a) R. Kuwano, K. Kaneda, T. Ito, K. Sato, T. Kurokawa, Y. Ito, *Org. Lett.* **2004**, *6*, 2213–2215; b) R. Kuwano, M. Kashiwabara, K. Sato, T. Ito, K. Kaneda, Y. Ito, *Tetrahedron: Asymmetry* **2006**, *17*, 521–535; c) A. M. Maj, I. Suisse, C. Méliet, F. Agbossou-Niedercorn, *Tetrahedron: Asymmetry* **2010**, *21*, 2010–2014; d) N. Mršić, T. Jerphagnon, A. J. Minnaard, B. L. Feringa, J. G. de Vries, *Tetrahedron: Asymmetry* **2010**, *21*, 7–10; e) R. Kuwano, M. Kashiwabara, *Org. Lett.* **2006**, *8*, 2653–2655; f) A. Baeza, A. Pfaltz, *Chem. Eur. J.* **2010**, *16*, 2036–2039; g) D.-S. Wang, J. Tang, Y.-G. Zhou, M.-W. Chen, C.-B. Yu, Y. Duan, G.-F. Jiang, *Chem. Sci.* **2011**, *2*, 803–806; h) Y. Duan, M.-W. Chen, Z.-S. Ye, D.-S. Wang, Q.-A. Chen, Y.-G. Zhou, *Chem. Eur. J.* **2011**, *17*, 7193–7197; i) Y. Duan, M.-W. Chen, Q.-A. Chen, C.-B. Yu, Y.-G. Zhou, *Org. Biomol. Chem.* **2012**, *10*, 1235–1238.
- [27] a) R.-H. Fish, A. D. Thormodsen, G. A. Cremer, *J. Am. Chem. Soc.* **1982**, *104*, 5234–5237; b) R. A. Sanchez-Delgado, D. Rondon, A. Andriollo, V. Herrera, G. Martin, B. Chaudret, *Organometallics* **1993**, *12*, 4291–4296; c) M. Rosales, R. Vallejo, J. Soto, L. Bastidas, K. Molina, P. Baricelli, *Catal. Lett.* **2010**, *134*, 56–62; d) C. Bianchini, P. Barbaro, M. Macchi, A. Meli, F. Vizza, *Helv. Chim. Acta* **2001**, *84*, 2895–2923.
- [28] E. M. Vogl, H. Gröger, M. Shibasaki, *Angew. Chem.* **1999**, *111*, 1672–1680; *Angew. Chem. Int. Ed.* **1999**, *38*, 1570–1577.
- [29] a) F. Spindler, B. Pugin, H.-U. Blaser, *Angew. Chem.* **1990**, *102*, 561–562; *Angew. Chem. Int. Ed. Engl.* **1990**, *29*, 558–559; b) T. Morimoto, N. Nakajima, K. Achiwa, *Chem. Pharm. Bull.* **1994**, *42*, 1951–1953; c) K. Satoh, M. Inenaga, K. Kanai, *Tetrahedron: Asymmetry* **1998**, *9*, 2657–2662; d) D. Xiao, X. Zhang, *Angew. Chem.* **2001**, *113*, 3533–3536; *Angew. Chem. Int. Ed.* **2001**, *40*, 3425–3428; e) H.-U. Blaser, H.-P. Buser, R. Haeusel, H.-P. Jalett, F. Spindler, *J. Organomet. Chem.* **2001**, *621*, 34–38; f) B. Pugin, H. Landert, F. Spindler, H.-U. Blaser, *Adv. Synth. Catal.* **2002**, *344*, 974–979; g) R. Dorta, D. Broggi, R. Stoop, H. Ruegger, F. Spindler, A. Togni, *Chem. Eur. J.* **2004**, *10*, 267–278.
- [30] K. Tani, J. Onouchi, T. Yamagata, Y. Kataoka, *Chem. Lett.* **1995**, *24*, 955–956.
- [31] a) G. Szollosi, Z. Makra, M. Bartok, *React. Kinet. Catal. Lett.* **2009**, *96*, 319–325; b) Z. Makra, G. Szollosi, M. Bartok, *Catal. Today* **2012**, *181*, 56–61.
- [32] T. Y. Kim, T. Sugimura, *J. Mol. Catal. A Chem.* **2010**, *327*, 58–62.
- [33] See the Supporting Information.
- [34] For a review on Hantzsch esters, see: S. G. Ouellet, A. M. Walji, D. W. C. MacMillan, *Acc. Chem. Res.* **2007**, *40*, 1327–1339.
- [35] a) M. Rueping, A. P. Antonchick, T. Theissmann, *Angew. Chem.* **2006**, *118*, 3765–3768; *Angew. Chem. Int. Ed.* **2006**, *45*, 3683–3686; b) D.-W. Wang, W. Zheng, Y.-G. Zhou, *Tetrahedron: Asymmetry* **2007**, *18*, 1103–1107; c) Q.-S. Guo, D.-M. Du, J. Xu, *Angew. Chem.* **2008**, *120*, 771–774; *Angew. Chem. Int. Ed.* **2008**, *47*, 759–762; d) M. Rueping, F. Tato, F. R. Schoepke, *Chem. Eur. J.* **2010**, *16*, 2688–2691; e) M. Rueping, T. Theissmann, M. Stoeckel, A. P. Antonchick, *Org. Biomol. Chem.* **2011**, *9*, 6844–6850; f) T. B. Nguyen, H. Bousserouel, Q. Wang, F. Guéritte, *Adv. Synth. Catal.* **2011**, *353*, 257–262; g) T. B. Nguyen, Q. Wang, F. Guéritte, *Chem. Eur. J.* **2011**, *17*, 9576–9580; h) Y. Zhao, Q. Liu, J. Li, B. Zhou, *Synlett* **2010**, 1870–1872.
- [36] a) M. K. Hays, R. Eisenberg, *Inorg. Chem.* **1991**, *30*, 2623–2630; b) H. E. Selnau, J. S. Merola, *Organometallics* **1993**, *12*, 3800–3801; c) J. D. Feldman, J. C. Peters, T. D. Tilley, *Organometallics* **2002**, *21*, 4050–4064; d) D. Carmona, J. Ferrer, M. Lorenzo, M. Santander, S. Ponz, F. J. Lahoz, J. A. López, L. A. Oro, *Chem. Commun.* **2002**, 870–871; e) C. Tejel, M. A. Ciriano, S. Jiménez, L. A. Oro, C. Graiff, A. Tiripicchio, *Organometallics* **2005**, *24*, 1105–1111; f) T. Hara, T. Yamagata, K. Mashima, Y. Kataoka, *Organometallics* **2007**, *26*, 110–118; g) M. Liniger, B. Gschwend, M. Neuburger, S. Schaffner, A. Pfaltz, *Organometallics* **2010**, *29*, 5953–5958.
- [37] a) R. Noyori, S. Hashiguchi, *Acc. Chem. Res.* **1997**, *30*, 97–102; b) K.-J. Haack, S. Hashiguchi, A. Fujii, T. Ikariya, R. Noyori, *Angew. Chem.* **1997**, *109*, 297–300; *Angew. Chem. Int. Ed. Engl.* **1997**, *36*, 285–288; c) M. Yamakawa, H. Ito, R. Noyori, *J. Am. Chem. Soc.* **2000**, *122*, 1466–1478; d) R. Noyori, T. Ohkuma, *Angew. Chem.* **2001**, *113*, 40–75; *Angew. Chem. Int. Ed.* **2001**, *40*, 40–73; e) C. A. Sandoval, T. Ohkuma, K. Muniz, R. Noyori, *J. Am. Chem. Soc.* **2003**, *125*, 13490–13503; f) S. Glialdi, E. Alberico, *Chem. Soc. Rev.* **2006**, *35*, 226–236.
- [38] R. Dorta, P. Egli, F. Zürcher, A. Togni, *J. Am. Chem. Soc.* **1997**, *119*, 10857–10858.

- [39] a) A. L. Casalnuovo, J. C. Calabrese, D. Milstein, *J. Am. Chem. Soc.* **1988**, *110*, 6738–6744; b) J. Zhou, J. F. Hartwig, *J. Am. Chem. Soc.* **2008**, *130*, 12220–12221. 584–589; d) *Amplification of Chirality* (Ed.: K. Soai), Springer-Verlag, **2008**; e) L. Schiaffino, G. Ercolani, *Angew. Chem.* **2008**, *120*, 6938–6941; *Angew. Chem. Int. Ed.* **2008**, *47*, 6832–6835.
- [40] a) K. Soai, T. Shibata, H. Morioka, K. Choji, *Nature* **1995**, *378*, 767–768; b) D. K. Kondepudi, K. Asakura, *Acc. Chem. Res.* **2001**, *34*, 946–954; c) D. G. Blackmond, *Tetrahedron: Asymmetry* **2006**, *17*,

Received: April 21, 2012  
Published online: August 22, 2012